Gravel for Salmon in Bedrock Channels: Elucidating Mitigation Efficacy Through Site Characterization, 2D-Modeling, and Comparison Along the Yuba River, CA

By

AARON ANDREW FULTON
B.S. (University of California, Davis) 2005

Thesis

Submitted in partial satisfaction of the requirements for the degree of

Master of Science

in

Hydrologic Sciences

in the

OFFICE OF GRADUATE STUDIES

of the

UNIVERSITY OF CALIFORNIA

DAVIS

Approved:

Gregory B. Pasternack, Professor of Hydrologic Sciences

Jeffrey Mount, Professor of Geology, Director of the Center for Watershed Sciences

---

Hamish J. Moir, Phd., Macaulay Institute, Aberdeen, UK

Committee in Charge

2008

(Page Intentionally Left Blank)

Aaron Andrew Fulton
October 2008
Hydrologic Sciences

Gravel for Salmon in Bedrock Channels: Elucidating Mitigation Efficacy Through Site Characterization, 2D-Modeling, and Comparison Along the Yuba River, CA

ABSTRACT

Aside from blocking upper watershed spawning areas, dams degrade in-stream aquatic habitat conditions by reducing or halting the transport of alluvial sediments that some species like salmon require for spawning. Gravel augmentation (GA), the technique of adding gravels to regulated rivers directly below impoundments, attempts to restore alluvial sediment inputs and has produced high quality interim spawning habitat in many gravel-bed channels since the 1970s. In the future, as Federal Energy Regulatory Commission permits are reissued, GA could be used as mitigation for upstream habitat loss and as a way to bolster declining populations. Although a significant effort has been made to develop channel rehabilitation programs that include GA on low gradient gravel-bed channels, no previous studies have investigated the role and applicability of GA in bedrock channels.

In this study, we evaluated the efficacy of GA in a bedrock channel below Englebright Dam on the Yuba River, CA using historical imagery, surface grain measurements, 2-D hydrodynamic modeling, habitat suitability curves, sediment transport analyses, and inter-site comparisons. Overall we tested nine hypotheses related to sediment characteristics, hydraulics, geomorphology, and spawning habitat to elicit controls on GA in bedrock channels.

The sediment size distribution at the Englebright Darm Reach (EDR) is significantly coarser than the highly utilized Timbuctoo Apex Reach (TBAR) and can be improved through GA. While a velocity reversal and flow convergence routing promote riffle pool maintenance at the alluvial TBAR, no reversal was observed at the EDR. Instead, lateral and vertical constrictions associated with the underlying bedrock morphology at the EDR create convergence along topographical highs and divergence within pools for all discharges. Therefore, flow convergence routing at the EDR will tend to fill existing pools with augmented gravels or lead to particle accumulation along channel margins where depositional features impact local hydraulics. Shields stress predictions at the EDR suggest the entire channel is stable during spawning flows and that full transport of augmented gravels can be expected in the channel center at discharges above 900.5 m^3/s (5-yr event). A consistent pattern of maximum velocity and Shields stress in the channel center will prohibit the formation of cross channel alluvial habitat. Overall, small scale GA in bedrock channels similar to the EDR will lead to small improvements in suitable habitat instead of macro-scale spawning beds and riffles constructed in regulated gravel bed channels. The greatest increase in habitat quality will occur along channel margins where roughness features in the channel promote deposition.

ACKNOWLEDGEMENTS

First, I would like to thank Gregory Pasternack and his previous graduate students Chien Wang, Joe Merz, Joe Wheaton, Eve Elkins, Rocko Brown, and Marisa Escobar. Their efforts and additions to the methodologies employed herein made this project possible. Funding was provided by the U.S. Fisheries and Wildlife Service (Award # 113323J011 and 813325G004) while Diana Cummings and Tania Guilfoil of the UC Davis Center for Watershed Sciences provided administrative support. Extensive site access was granted by Curt Aikens and staff at the Yuba County Water Agency, Doug Grothe of the U.S. Army Corps., Ralph Mullican, and the University of California Browns Valley Research Station. Field and technical support was provided by James Kulpa of Environmental Data Solutions and Scott Morford. I would also like to thank Greg Pasternack, Jeff Mount, Hamish Moir, and Peter Moyle for stimulating my interest in geomorphology and salmonid ecology and providing inspiration for my own research. Finally, I am indebted to my family, Harold and Tish Fulton, Deborah and Kevin Kalkowski, Frank and Barbara Caliva, Shannon Fulton, and Dana Jewell for their unwavering support and patience.

1. INTRODUCTION

Dams throughout California and the Pacific Northwest suppress anadromous salmonid populations by blocking access to historic spawning areas and severing the hydrologic, geomorphic, and ecologic continuity that river ecosystems require (Baxter, 1977; Brandt, 2000; Bunn and Arthington, 2002; Collier et al., 1996; Graf, 1999; Ligon et al., 1995; Poff et al., 1997; Power et al., 1996; Williams and Wolman, 1984). The initial tool for mitigating the effects of dams on fisheries was grounded in an industrial/agricultural vision that embraced fish hatcheries as a technology that could produce water, power, agriculture, and salmon from the worlds' rivers (Lichatowich 1999). Despite a federally supported hatchery program, the decline of Pacific salmon stocks continued and fueled further investigation and development of mitigation measures like fish ladder/transport systems (Cada and Sale, 1993), sub-thermocline water releases (Crisp, 1987), re-regulated flow regimes (Richter, 2007; Ward and Stanford, 1995), and spawning habitat rehabilitation projects (SHR) that use channel design in combination with gravel augmentation (GA) to increase spawning habitat (Bunte, 2004).

GA entails adding spawning sized gravels to degraded channels to improve aquatic habitat. It can be effective at increasing the quantity and quality of physical habitat for multiple salmonid life stages on highly regulated, low gradient, gravel-bed rivers where physical habitat quality is defined as the degree of suitability of local depth, velocity, and river-bed substrate size in a stream to support a particular ecological function (e.g., spawning, rearing) (CDWR, 1992; Elkins et al., 2007; Merz, 2006; Merz et al., 2004; Mesick, 2002). Using GA to shift physical habitat quality from poor to high has been

tested experimentally and found to increase fish utilization of previously degraded aquatic channels (Elkins et al., 2007).

However, the effectiveness of GA has not been investigated below dams in bedrock channels, where the character and pattern of ongoing physical processes are substantially different from low gradient gravel-bed rivers. In particular, bedrock channels often have high transport capacity and low sediment supply which promote redd scour or may limit the production of suitable spawning habitat within a reach. If GA is selected as mitigation for habitat loss upstream of dams or used to increase in-stream habitat quality to meet fisheries goals in bedrock channels, the overall effectiveness must be determined before widespread adoption in the public and legal arena transpires.

To bridge the void between GA in alluvial and bedrock channels this study set out to determine the potential benefit of GA by characterizing and comparing the substrate, depth, velocity, and sediment transport regimes of two study sites; (1) a bedrock channel, and (2) an alluvial reach, both on the lower Yuba River (LYR), CA. The study uses established empirical, numerical, and analytical methods to predict the overall efficacy of an established rehabilitation tool in a novel environment.

1.1. Bedrock Channels

Of the ten large anadromous fish bearing tributaries in the Sacramento/San Joaquin Delta system, the Stanislaus, Sacramento, Feather, Yuba, and Calaveras Rivers contain a continuous stretch (>0.5 km) of bedrock channel below an impassable barrier. Bedrock channels have been loosely defined as those with >50% exposed bedrock and include reaches with a hydraulic and morphologic character controlled by resistant underlying

geologic formations (Wohl and Tinkler, 1998). In reality, the number of anadromous rivers in California that experience some form of bedrock control at higher discharges is much greater, as bedrock reaches also occur on the Tuolumne and Merced Rivers.

Differences in physical processes between bedrock and gravel-bed channels must be considered prior to GA. Bedrock channels are more efficient at moving sediment because they typically exhibit a reduced valley width, high gradient, and higher average velocity than their lowland alluvial counterparts (Wohl and Tinkler, 1998). In general, transport capacity generally exceeds sediment supply in bedrock channels (i.e. they are supply limited) which suggests that bedrock reaches function as sediment routing units and have limited capacity to retain coarse sediments. This differs significantly from alluvial channels where coarse sediments compose the entire channel bed. The response to discharge in alluvial and bedrock channels is also different. Alluvial channel morphology is controlled by more frequent events with a one to five year return interval that rearrange the water-sediment boundary (Emmett and Wolman, 2001), but bedrock channel morphology is controlled by lower frequency events that create the hydraulics and grain ballistics necessary to lift bedrock slabs, abrade bedrock, and move boulders and wood through the channel (Whipple, 2001)

These disparities suggest that the observed processes and outcomes associated with GA efforts in alluvial channels should be carefully evaluated for the potential effectiveness in bedrock channels. For example, MacWilliams (2006) proposed that flow convergence over riffles in alluvial channels during long periods of low flow causes armoring, gradual incision, and diminishing relief. However, during high magnitude and infrequent floods flow convergence shifts to pools, causing pool scour, deposition near

riffles, and enhancement of overall relief. This proposition is based on Keller (1971), who observed higher near bed velocities and shear stress in pools than riffles during high flows. It is unclear whether flow convergence routing in bedrock channels is responsible for observed patterns of thin alluvial deposits there, and thus salmon habitat distribution.

Because an understanding of geomorphic processes in bedrock channels is required for GA, further investigation into the dominant mechanisms of habitat formation is warranted and should be based on previous research. McBain (2004) proposed that "nested depositional features", including large immobile boulders, channel spanning bedrock formations, and large wood, control gravel deposition in bedrock channels at multiple scales. In another study Wohl (1998) coined the term "gravel beaches" which referred to the depositional environments behind large boulders and topographic highs. Overall, these studies provide a conceptual basis for predicting bedrock channel response to GA and its potential use as a sustainable river rehabilitation tool.

1.2. Gravel Augmentation

GA introduces coarse gravels within or along a channel with the intention that future flows will entrain, transport, and deposit sediments downstream: ideally to yield some form of usable habitat for spawning salmonids. It first surfaced in late 1960s as a tool for the rehabilitation of salmonid spawning habitat and replenishment of coarse sediment deficiencies below large dams that cut off sediment inputs (Kondolf, 2004). In fact, since 1968 over 380,000 m^3 of gravel have been added to California rivers in projects of varying success (Minear and Kondolf, 2006). Overall, this method of habitat rehabilitation is more conducive for rivers with high bed slopes and periodic overbank

flows capable of reworking coarse sediment annually or biennially. Therefore, an understanding of hydraulics and sediment transport is required in GA projects because the hydrogeomorphic regime determines the fate of introduced gravels.

GA attempts to re-instate geomorphic continuity and mitigate for some of the physical channel modifications linked to dams. This includes incision, substrate coarsening, bank stabilization, habitat homogenization, channel narrowing, and a lack of spawning gravels for anadromous species (Brandt, 2000; Friedman et al., 1998; Kondolf, 1997; Williams and Wolman, 1984). The damming of rivers also endangers salmonids through flow and temperature regime alterations, dissolved oxygen reductions, loss of in-stream wood habitat, vegetation encroachment, and abrupt changes in macro invertebrate assemblages (NMFS, 2006). As a habitat rehabilitation tool GA aims to alleviate sediment deficiencies, reduce incision, promote floodplain connectivity, increase hyporheic flow and dissolved oxygen content, increase interstitial habitat for benthic macro invertebrate populations, and provide substrate for redd construction (Merz, 2005). For instance, after studying the gravel bed Clackamas River in Oregon, Grant (2006) showed that bars formed by augmented gravels promoted lateral hyporheic flow and reduced diurnal temperature extremes experienced by salmonids.

GA involving annual injections in perpetuity is a decadal to centennial scale rehabilitation tool because the passive creation of habitat and associated geomorphic features (riffles, pools, bars, lateral shear zones) may take a long time to occur. GA relies on flows to redistribute sediments and create such features and therefore, increases in habitat quantity and quality are unlikely to result if flows do not redistribute gravels, if the amount of introduced gravel is less than channel deficits, or if annual transport

exceeds augmentation rates. GA is unique in that a design based on a specific flow or channel prototype (Rosgen, 1985) is not used. Instead, GA reinstates sediment supply and relies on the remaining dynamism of a regulated system to mimic process rather than form (Stanford et al., 1996; Wohl et al., 2005). It is uncertain whether sufficient dynamism remains in a degraded river to achieve the desired goals or whether GA could be yet another harmful ecological disturbance.

1.3. Spawning Habitat Rehabilitation

Spawning habitat rehabilitation (SHR) is a sub-type of GA that includes direct manipulation of channel morphology via design and modeling programs to create specific areas of high quality spawning habitat and/or jumpstart geomorphic processes that cleanse gravels (Wheaton et al., 2004a; Wheaton et al., 2004b). Therefore, the persistence and success of SHR projects is highly dependent on design considerations and geomorphic thresholds that when exceeded may change a rehabilitation site or scour redds during embryo development (Kondolf, 1998; Merz, 2006). SHR, which includes riffle construction, hydraulic structure placement, and slope creation, is the primary management tool for quickly mitigating geomorphic and hydrologic discontinuities in regulated rivers and increasing the quality and quantity of spawning habitat in the near term (Elkins et al., 2007; Kondolf, 2004; Wheaton, 2004). Projects have been completed on rivers throughout California and the Pacific Northwest, including the Sacramento, Mokelumne, Stanislaus, Tuolumne, Merced, and Trinity Rivers in California, and the Clackamas River in Oregon (Grant et al., 2006). SHR has been implemented

internationally with projects in Newfoundland (Scruton, 1996), the United Kingdom (Harper et al., 1998), and Germany (Zeh and Donni, 1994).

1.4. Habitat Rehabilitation Constraints

GA and SHR projects face the same constraints that fish hatcheries contended with in the 1900s. A lack of funding for pre and post-project evaluations that test project objectives clouds the overall understanding and applicability of these projects (Kondolf, 1998; Kondolf, 2001). The most scientifically valuable studies are those with clear objectives and testable hypotheses. For example, Merz (2005) analyzed measurable habitat characteristics such as dissolved oxygen, inter-gravel flow, invertebrate populations, and substrate conditions before and after a rehabilitation project on the Mokelumne River, CA. Two testable hypotheses in GA projects include (1) was suitable habitat created over the time scale of interest? and (2) was habitat sufficiently used by salmon to warrant expenditures? Tests of the two hypotheses would include measuring the areal extent of habitat following transport events and annual redd surveys downstream of gravel injection sites to monitor habitat utilization. Pre-project data synthesis and post-project analysis would provide an appropriate arena for evaluating GA studies that try to elucidate patterns of gravel transport, morphologic change, habitat formation, possible redd scour, and overall effects on the freshwater life stages of anadromous fish. However, given cost constraints and shifting priorities of many rehabilitation programs, the post-project monitoring necessary for testing hypotheses is often not prioritized

Based on a national survey of 37,099 projects, Bernhardt et al. (2005) estimated that over $1 billion/yr is spent on restoration projects of varying objectives. Kondolf (1998)

suggested that objectives based on an ecologic and geomorphic understanding at the reach and basin scale are essential for project success. This parallels the view of Ebersole (1997) who proposed that habitat expression is a complex function of stratified systems spanning four and seven orders of magnitude in spatial and temporal processes, respectively. An attempt to understand the processes controlling habitat formation and rehabilitation should consider these scales and begin with a historic and contemporary biogeomorphic analysis of the targeted watershed (Kondolf, 1995). This includes evaluating basin hydrologic events with available streamgage data, estimating sediment transport, and accounting for anthropogenic forcing due to mining, road building, agriculture, etc. Important reach-scale processes and characteristics include the quantity, quality, and spatial distribution of sediment, channel form, mass wasting, valley confinement and expansion, channel response (depth, width, velocity, bed shear stress) to increasing discharge, and anthropogenic boundary controls (Brown and Pasternack, 2008). When combined, these processes and characteristics determine the physical habitat encountered by a target species such as Chinook salmon (*Oncorhynchus thyswatcha*) and Steelhead trout (*Oncorhynchus mykiss*).

The underlying goal of anadromous habitat rehabilitation projects, whether SHR or GA, is to increase escapement. Therefore, a full understanding of life history characteristics and habitat requirements of the target species is critical. An evaluation of species population history, type, run timing, lotic habitat requirements, and possible physical limitations to biologic productivity is essential. For example, if pre-project studies suggest available spawning habitat is not limiting at a site, then habitat restoration targeting juvenile rearing habitat may be more appropriate than GA or hydraulic structure

placement. If pre-project analysis and modeling show unsuitable combinations of substrate size, flow velocity, and depth, GA directed at spawning habitat improvement may be beneficial. In other words, habitat rehabilitation will be most successful when watershed managers approach projects with both ecologic and geomorphic information in hand.

To generate this information and overcome rehabilitation constraints for the case of bedrock channels, this study combines a traditional geomorphic approach with 2-D numerical simulations of channel hydraulics that have been used to test channel designs, conceptualize ongoing physical processes, and select appropriate sites for GA in numerous SHR projects (Bunte, 2004; Wheaton et al., 2004a; Wheaton et al., 2004b). For example, when combined with high quality digital elevation models (DEMs), sediment transport, habitat suitability, and overall site hydraulics can be approximated with widely available hydraulic models (e.g. MIKE-21, RMA2, UnTRIM, FESWMS, SHR-2D, and TELEMAC) to determine where GA might be effective (Rathburn and Wohl, 2003).

2. OBJECTIVES

The overall goal of this study was to elucidate the efficacy of GA as a habitat mitigation tool in the bedrock Englebright Dam Reach (EDR) of the LYR, CA by characterizing and comparing it against a highly utilized spawning reach in the alluvial portion of the same river. The specific objectives were to: 1) quantify bed material and local hydraulic patterns with traditional sediment characterization protocols and a 2-D hydrodynamic model, 2) assess the historic and current hydrogeomorphic regimes by

analyzing hydrologic patterns, historical imagery, approximating sediment transport patterns, and modeling contemporary instream Shields stress, and 3) map the current spatial pattern of spawning habitat with habitat suitability curves for each site. Comparisons of qualitative and numerical data at each site were used to test specific hypotheses related to GA efficacy in bedrock channels **(Table 1)**. The significance of this study is that it provides a process-based approach for determining the applicability of an increasingly popular regulated river rehabilitation tool in bedrock channels. A secondary yet important benefit of this approach is the substantive baseline information required for adaptive management and determination of gravel augmentation project success.

3. STUDY SITE

3.1. Watershed Attributes

The Yuba River watershed, located northeast of Sacramento on the western flank of the Sierra Nevada, encompasses 3480 km² of topographically diverse vegetated landscapes **(Fig. 1)**. In the upper watershed bedrock lined canyons drain glacially cut granitic plutons formed as the Pacific plate subducted the North American plate approximately 80 million years ago. The geology of the lower watershed is more heterogeneous, including overlapping belts of shale, sandstone, metavolcanics, and highly metamorphosed combinations thereof (Hill 2006). The watershed experienced three late Pleistocene glacial episodes, each depositing significant amounts of cobble and gravel along the Sierra Nevada front where reduced slopes promoted deposition (James, 2002). These transitional and highly active meandering river environments were

exploited by numerous species of Pacific salmon as they evolved in a rapidly changing geologic environment (Montgomery, 2000).

The current Mediterranean climate, with precipitation exceeding 1500 mm in higher elevations and 500 mm in the lower watershed, controls basin hydrology. Winters are cool and wet with an occasional tropical influence, while summers are dry and hot. Ambient air temperatures frequently exceed 35ºC (95 ºF) during the summer months and fall below freezing (0 ºC) in many parts of the upper watershed during the winter. A combination of a cooling gradient towards higher elevations and an orographic effect causes most precipitation to fall in the upper watershed as snow between the months of December and April. This spatial diversity of geology, precipitation, and temperature regimes has sustained mixed coniferous forests (*Pinus, Calocedrus, Abies*) at high elevations (>1000 m) , and oak (*Quercus spp.*) woodlands, chaparral (*Ceanothus spp., Chamise spp.*), Manzanita (*Arctostaphylos spp.*), willow (*Salix spp.)*, alder (*Alnus spp.*), and cottonwood (*Populus spp.*) populations along the Sierra front where the study site is located.

With an average annual unimpaired run-off of 3.02 km³ (2.25 maf), the Yuba basin is a snowmelt system that historically peaked between the months of April and July. Together the north (1270 km²), middle (543 km²), and south (1010 km²) fork drainages have experienced significant human alterations, including projects by local irrigation districts, Pacific Gas and Electric, and the Yuba River Development Project administered by the Yuba County Water Agency. The cumulative effects of five dams, water diversions, logging, mining, and other land use changes have drastically altered the physical, chemical, and thermal habitat characteristics of the basin's lotic systems.

However, water temperatures in the main stem of the Yuba are cool enough, due to sub-thermocline reservoir releases, to sustain one of the last remaining hatchery-free runs of Chinook salmon (spring and fall runs) and Steelhead trout in California. This unique natural assemblage of anadromous salmonids, a vestige of a once prolific annual ecologic cycle that connected ocean productivity to inland food webs, supplemented First Peoples' diets and later supported an influx of miners after the discovery of gold in 1848 (Yoshiyama et al., 1998).

Gold mining in the Yuba watershed completely altered geomorphic processes with additions of hydraulic mining debris, channel obstructions, and increased fine sediment loads (Mount 1995; James 1999; James 2005; Snyder 2006). Early miners relied heavily on panning and sluice box sorting to locate gold within and adjacent to stream channels. However, as these surficial placer deposits waned a new method called hydraulic mining was employed to target tertiary gravels in ancient riverbeds. Hydraulic mining leveled hillsides and deposited far more sediment into Yuba River tributaries than stream networks could transport. The single largest delivery of sediment to the Sacramento River watershed, (~522 million m^3), originated in the South Fork of the Yuba River where hydraulic mining was particularly extensive (Gilbert 1917 quoted in (James, 2005)). The resulting channel aggradation, of up to 40 m, impacted river morphology and continues to control lotic community composition more than a century after hydraulic mining was discontinued.

In 1884 the Sawyer Decision temporarily terminated large scale hydraulic mining in the Yuba Basin and across California. The law aimed to reduce flood damage to crops and personal property caused by hydraulic mine debris that reduced levee system

capacity in the farming communities of Yuba City and Marysville to the west. However, 9 years later, the Caminetti Act re-authorized this devastating technique through a permit and inspection program loosely administered by federal government. James (2005) investigated the historical influx of hydraulic mining debris in the Yuba Watershed before and after the Sawyer Decision. This work suggests the effects of historic hydraulic mine operations have been largely misunderstood and concealed by erroneous and inadequate record keeping. In reality, large-scale damage to Yuba River fisheries continued into the 1950s, well after public outcry inadvertently provided environmental protection. Unfortunately fisheries endured further stress with the construction of sediment barriers and reservoirs for California's growing water demand.

3.2. Dams and Discontinuities

Englebright Dam, with a capacity of 86 million m^3, was completed in 1941 to halt hydraulic mining sediments, reduce levee infilling, and mitigate flood levels for farmers in the rapidly growing agricultural communities to the west. At 81 m high, the concrete arch structure with an ogee crested spillway has caused both ecologic and physical system discontinuities. The dam currently blocks anadromous fish access to historic upper-watershed spawning areas and limits habitat to the LYR, a 39 km stretch between Englebright and the Feather River confluence.

Englebright Dam physically separates the Yuba River basin into two geomorphically independent units. The transport of coarse sediment from the upper watershed is completely blocked from the LYR. Suspended silt and clay as well as wood can float over Englebright Dam, but these mostly flush out to the Feather River. A bathymetric

survey of Englebright reservoir by Snyder (2004) estimated that 24,000,000 metric tons of total sediment, including 4,728,700 metric tons of coarse cobble and gravel, has accumulated between 1941 and 2004 and reduced reservoir capacity by almost 25%. These coarse sediments, a combination of natural load and hydraulic mining debris, are presently locked within the reservoir creating a major geomorphic discontinuity. Although significant in-channel, bar, and remnant dredge tailing gravel sources exist within 3 km of Englebright Dam, near complete cessation of gravel recruitment to the EDR has occurred; gravel that is key for salmon survival.

Englebright Dam is situated below the largely unregulated south and middle forks of the Yuba, provides minimal flood protection, and is designed to overtop in most years. Given the small capacity of the lake, Englebright Dam was unable to attenuate major floods in 1950, 1986, and 1997 for the communities of Marysville and Yuba City. Englebright reservoir is home to a small year round house boat and small summer recreational boating community and produces $10 million in hydropower each year (Pejchar 2001). These varying anthropocentric benefits are far reaching, but have impacted anadromous salmonid populations throughout the watershed by cutting off key upper-watershed habitat of the threatened spring run Chinook salmon.

Damming of the middle and south forks of the Yuba River above Englebright reservoir has created numerous small reservoirs at the highest elevations in these sub-basins. The reservoirs have small contributing areas and influence summer flows and water temperatures during dry years. Spaulding reservoir (92.6 million m^3) is larger than Englebright and was completed in 1913 at an elevation of 1528 m by Pacific Gas & Electric for hydropower production on the Yuba's south fork. In 1927 Canyon Creek, a

small tributary of the South Fork of the Yuba, was dammed by Nevada Irrigation District (NID) for drinking and irrigation purposes, forming Bowman reservoir at an elevation of 1642 m with a capacity of 84.5 million m^3. Jackson Meadows, the fourth largest dam upstream of Englebright at 77 million m^3, was completed in 1965 by NID at an elevation of 1840 m. Many other minor dams dot the Yuba watershed but their small size has a minor influence on hydrology relative to New Bullard's Bar Dam.

New Bullards Bar Dam was completed in 1969 and is situated 28 km upstream of Englebright on the North Fork Yuba. With a capacity of 1.2 billion m^3, its completion marked a shift in hydrograph properties of the basin **(Fig. 2)**. Long term USGS records for Smartville gages (#11418000 and #11419000) located approximately 500 m downstream of Englebright Dam allow an analysis of hydrologic alterations attributed to New Bullards bar using the non-parametric form of Indicators of Hydrologic Alteration (IHA) (Richter et al., 1996; Richter, 1997). Numerous deviations in biologically relevant hydrograph parameters include increased base flows, spawning flows, fall rates, and the number of discharge reversals **(Fig. 3)**. Flows in July, August, September, October, and November, corresponding to when adult salmon typically inhabit the Yuba, are between 1.5 and 2 times larger after New Bullards Bar was constructed. Increased fall rates, where discharge drops rapidly, and discharge reversals can cause juvenile stranding, redd drying, and sufficiently alter hydraulic conditions for both juveniles and adults such that survival can be compromised.

The hydrologic alterations suggested by IHA are consistent with flood frequency analysis comparing pre and post Bullards Bar flood regimes. Discharge records at the Smartville gage show that, typical of many regulated rivers, flood-peak dampening is

greatest for small events **(Fig. 4)**. Bullards Bar caused a 71% decrease in statistical bankfull discharge ($Q_{1.5}$) at Smartville from 590 m^3/s to 170 m^3/s. However, flows exceeding 590 m^3/s have occurred in 13 of 34 years since construction; suggesting a moderate dynamism (flood regime) still exists in the system. As demonstrated by morphological changes evident in the sequence of available historical photos and repetitive topographic surveying to be presented later, geomorphically significant flows capable of transporting and reworking remnant hydraulic mine deposits that once filled the river valley still occur.

3.3. Lower Yuba River

The first 3 km of the LYR is a bedrock dominated reach, while the lower 36 km is composed of a gravel-cobble bed channel. Historic additions of hydraulic mine debris significantly aggraded the entire LYR and since the construction of Engebright, an overall pattern of incision prevails throughout the LYR. Two small regulated tributaries, Deer and Dry creeks, join the Yuba 1.5 km and 16 km downstream of Englebright, respectively, and support small steelhead and Chinook salmon populations in their lower reaches. The hydrograph response to rainfall events is rapid in Deer and Dry Creeks, with flow event peaks occurring well before peaks in the mainstem Yuba.

The LYR has been delineated into 6 reaches based on dominant channel morphology and importance to spawning salmonids- Englebright Dam, the Narrows, Timbuctoo Bend, Highway 20, Daguerre Dam, and Simpson lane reaches **(Fig. 1)**. The EDR includes the 1.5 km of river between the Narrows II powerhouse (39º14’23.95”N, 121º16’08.48”W) and Deer Creek (39º13’47.75”N, 121º16’45.24”W) where bedrock

constrained and supply limited channel morphology prevails **(Fig. 1F)**. This section contains the GA site detailed in this study. The Narrows extends for 1.5 km below Deer Creek and is characterized by steep adjacent valley walls, significant bedrock control, rapids, large boulders, and deep pools **(Fig. 1E)**. After exiting the Narrows, the river flows 6 km in the Timbuctoo Bend Reach (TBR), an active gravel bed zone with an abundant supply of coarse substrate from adjacent dredge tailing and hydraulic mine deposits **(Fig. 1D)**. Alternating bar, island, side channel, and pool complexes dominate the river from the Narrows exit, through the TBR to the Hwy 20 Bridge. The Hwy 20 reach begins at the bridge and extends 10 km to the Daguerre Point diversion dam **(Fig. 1C)**. Throughout the Hwy 20 reach, valley width is generally wider than portions of the river upstream of Hwy 20, thus the river is less confined by adjacent hillsides. Similar to TBR, the Hwy 20 reach contains numerous side channels and island complexes that transition into a divided morphology upstream of Daguerre Dam. Within the Hwy 20 reach the Yuba River is still adjusting to the elevation control imposed by Daguerre with numerous riffle knickpoints evident. However the exact boundary between the adjusted and unadjusted reach has not been delineated. The Daguerre Dam reach **(Fig. 1B)** contains numerous elongated lateral bars and limited side channels before transitioning into a deep, fine grained, levee constricted channel known as the Simpson Lane reach **(Fig. 1A)**, 11 km below Daguerre Dam. Willow species are the dominant vegetation type along channel edges throughout the TBR and Daguerre Dam reaches and provide essential habitat for beavers, salmonids, amphibians and a host of other aquatic and terrestrial species.

Typical spawning habitat along the main-stem Yuba is situated around pool exits/riffle entrances, side channels, and along margins near flow separation features (Moir and Pasternack, 2008). Site visits throughout the TBR section have demonstrated the ability of Chinook salmon to use very small areas (<1 m^2), however the majority of observed redds are clustered near pool exits and riffle entrances. Spawning habitat is most limited between Englebright Dam and the Deer Creek confluence where bed coarsening from dam construction and scour associated with significant floods (>2830 m^3/s) in 1963, 1965, 1986, 1997, and 2005 has likely occurred. The highest quantity of habitat is found within TBR and Hwy 20 reaches while the Daguerre Dam reach has slightly less area due to fewer riffles and side channels.

Two persistent anthropogenic structures inhibit adult and juvenile salmon populations on the LYR. The first is the Yuba Goldfields, a complex mosaic of active and historic gold/gravel dredge tailings and pools that pose a significant challenge to system management (Brown et al., 1998). This prevalent feature extends adjacent to the river from Browns Valley to 5.5 km beyond Daguerre Dam **(Fig. 1)**. Hyporheic flow between tailing pools and the river network complicate discharge analysis and alter water temperatures within the river. In the past, large floods have reconnected the channel to the Yuba Goldfields, allowing anadromous juveniles to stray into deep tailings pools where invasive warm-water species including black bass (*Micropterus salmoides)*, channel catfish (*Ictalurus punctatus)*, black crappie (*Pomoxis nigromaculatus*) and other centrarchid species are prevalent. When adult salmon and steelhead return from the ocean they negotiate the 2nd important structure. The 8.5 m high Daguerre Point Dam is a sediment detention and water diversion structure that has two inadequately designed fish

ladders that fail to attract migrating adults. Furthermore, during out-migration juveniles can become disoriented as they plunge over the structure into a large pool where invasive warm water piscivores are abundant. Recent progress has been made to construct barriers to cease juvenile straying into the goldfields and a passage system at Daguerre has been under consideration since 1988 (Talbert, 1999).

3.4. Yuba River Salmonids

Steelhead trout and Chinook salmon utilize the Yuba River for spawning, rearing, and migration. The life history characteristics of Pacific salmonids are extremely variable, dynamic, and dependent on geographic location (Groot and Margolis, 1991; Yoshiyama et al., 1998). Four distinct races of Chinook occupy the Sacramento river system although only two, a spring run and a fall run, utilize the Yuba River today (Banks et al., 2000). Annual escapement on the Yuba is dominated by the fall run and has averaged ~ 14,000 Chinook/yr with observable inter-decadal fluctuations between 1953 and 2006 **(Fig. 5)**. The fall run enters freshwater between mid September and November and spawns within weeks of arriving at spawning grounds. The spring run, a federally threatened species, enters freshwater between April and June and over-summers in cool pools before spawning in August and September. Before dams were constructed and migration routes severed, this life history strategy enabled the spring run to penetrate deep into the watershed when high flows from snowmelt made it possible to pass natural hydraulic structures that impeded the fall run.

A dramatic decline in spring run populations throughout California has been attributed to dams which block up to 80% of historic spawning sites. On the Yuba,

although Englebright and New Bullards Bar restrict access to 73 % of upper watershed spawning areas, a remnant population of less than 1000 spring salmon persists and must spawn within the lower limits of its historic extent. The resulting loss of geographic isolation has likely caused genetic mixing and most certainly increased the relative competition between the two stocks as observed on the Sacramento river by Slater (1963).

From a fisheries management perspective, the population and life history characteristics of spring run salmon on the Yuba are not well documented and pose a major challenge to management decisions in the basin. On-going screw-trap studies by the California Department of Fish and Game and United States Fish and Wildlife Service near Daguerre Dam are expected to produce key information about age, size, and timing of juveniles during outmigration. For the purposes of habitat rehabilitation and GA, the instream requirements (temperature, dissolved oxygen, depth, velocity, substrate conditions, large wood structure) of spring run are assumed to parallel that of the fall run however differences in feeding habits, habitat preferences, and movements likely exist. Despite these uncertainties, habitat rehabilitation based on an understanding of fall run habitat is a suitable approach, especially given its numerical robustness.

3.5. Study Reaches

3.5.1 Englebright Dam Reach

The EDR begins at the Narrows II powerhouse pool at the uppermost section of the LYR **(Fig. 1)**. The EDR extends for 135 m in a narrow supply limited bedrock canyon of relatively low slope (avg. 0.18%, 0.0018 m/m). The upper pool is a release bay for water used in hydroelectric power generation and provides important spring and fall run adult

salmon holding habitat during the late summer months **(Fig. 6A)**. The channel is constrained by steep sparsely vegetated canyon walls and bordered by a narrow, elevated, unnatural floodplain on the western edge. Substrate in the floodplain and within the channel is composed of bedrock and large irregular boulders (> 256 mm intermediate axis diameter) blasted from surrounding hill-slopes during the construction of the dam. Limited pockets of angular gravel and cobble sized particles exist within boulder crevices and boulder shadows and deter riparian shrub colonization. Overall, channel morphology is bedrock controlled, valley confined, and exhibits significant substrate alteration from human construction activities.

3.5.1. Timbuctoo Bend Apex Riffle: Functional Spawning Segment

The highly functional salmon-spawning reach in this study is located ~5 km downstream of Englebright Dam along the active gravel/cobble TBR reach of the LYR **(Fig. 6B)**. Available historic aerial photographs and recent topographic surveys after significant floods of the site, called the Timbuctoo Bend Apex Riffle (TBAR), depict a dynamic morphology dominated by a persistent pool/island/riffle complex. Willow species line the bank, corresponding to the water surface elevation at ~1600 m^3/s. A large dredge tailing pile abuts the active floodplain on the uppermost southern side of the river. The well connected floodplain extends to the valley walls and contains numerous secondary channels active during large flow events. The site is dominated by cobble (64-256 mm) and gravel (2-64 mm) sized sediments. Additionally, there are a few large boulders associated with two exposed bedrock features opposite one another in the

middle of the site. No SHR projects have occurred at the site and natural Chinook spawning activity is extensive.

3.6. Gravel Augmentation and the Yuba River

Despite recent interest in dam removal across the Pacific Northwest and California, the hydrologic and geomorphic dominance exerted by hydropower facilities similar to Englebright are likely permanent controls on salmonid populations. If salmon populations are to persist, resource managers must continuously mitigate for habitat loss and degradation in channels directly below dams (CDWR, 2006). The process of organizing mitigation plans will occur over the next 20 years as the Federal Energy Regulatory Commission reviews operation contracts and stipulates the mitigation measures to be invoked. For example, Englebright Dam enters review in 2013 and some form of gravel augmentation will likely be required.. During the relicensing process mitigation for spawning habitat loss in sediment starved bedrock controlled channels will be a topic of debate with no proven mitigation strategy or system for evaluating overall efficacy.

GA has been proposed as a mitigation measure below Englebright Dam on the Yuba River, CA where Chinook salmon habitats have declined due to a combination of dam construction, hydraulic mining, logging, road building, urbanization, and hydropower development. In the fall of 2007, the United States Army Corps of Engineers (USACE) performed a small (629 metric tons) pilot gravel injection intended to provide data to guide a future mitigation plan aiming to increase spring-run Chinook spawning habitat in

the 1.5 km length of river between the Narrows powerhouse II and Deer Creek confluence.

4. METHODS

To provide a baseline habitat, hydraulic, and geomorphic characterization for testing the hypotheses in **Table 1**, field data was acquired between August 2005 and 2007 at the EDR and TBAR. Substrate, topographic, hydraulic, biological, and visual data was collected for 2D hydraulic modeling, validation, and subsequent biogeomorphic analyses. Historical photographs, stream-gage measurements, field reconnaissance, government documents, and previous geomorphic studies of the basin provided further background data to guide a historical and contemporary hydrologic and geomorphic assessment of each site. Previous salmon habitat restoration projects have focused on gravel-bed channels and the wealth of information available on hydrogeomorphic and ecologic processes in that stream type. The data collected in this study supported a comparative analysis aimed at determining if the same processes exist in bed-rock channels.

Overall, six discharges of comparable magnitude were evaluated at both sites using a standard 2D (depth averaged) hydraulic model that estimated the spatial distribution of depth and velocity at the ~1-m scale. The flows modeled at the EDR were the 22.7, 33.7, 271.3, 710.7, 900.5, and 2588.2 m^3/s. TBAR model simulations were completed for the 21.2, 34.6, 267.8, 655.3, 998.4, and 3089.2 m^3/s events. Required model inputs for the six comparable discharges at the EDR and TBAR are provided in **Table 2**. Two extra model runs, in addition to the 21.2 m^3/s event, were completed for evaluating model performance at 18.4 and 31.2 m^3/s at the TBAR. Overall, a total of fourteen flow

scenarios were modeled between the two sites. Model predictions were used to estimate spawning habitat quality and Shields stress distributions at each discharge, and thus represent spawning and sediment transport regimes. Although 2-D models have not been tested much in bedrock channels, the bed slope in this case was suitably low (0.18%) and allowed the model to illuminate river processes relevant to proposed mitigation strategies.

4.1. Topography

Topographic data of the channel and floodplain constrains DEM formulation and subsequent 2-D hydraulic modeling. The number of bed elevation points required within deeper parts of the channel to accurately represent the sites challenged traditional surveying methods that are limited by the depth and velocity that a surveyor can wade. Therefore, a combination of boat-based bathymetric and robotic total station surveys was employed to provide the site characterization required by the models used in this study. Bathymetric surveys were conducted on August 27, and June 10, 2005 for the EDR and TBAR, respectively. Robotic total station surveys were conducted before and after the bathymetric surveys to fully characterize areas the boat could not access. Water surface elevation data, composed of projected coordinates and elevation values, was recorded for a range of flows during the 2006 water year (i.e. October 2005-September 2006) as boundary conditions for the hydraulic model used.

4.1.1. Bathymetric and Total Station Surveys

A bathymetric survey was conducted by a professional hydrographer (Environmental Data Solutions, San Rafael, CA) on a customized 4.2-m long Zodiac raft in accordance

with U.S. Army Corps of Engineers' rigorous Class 1 standards. Geographic positioning (± 1 cm) was attained with a Trimble 5800 Real-Time Kinematic (RTK) base station and 5700 series rover mounted to the customized vessel. Depth was measured using an Odom Hydrotrac Fathometer (3°, 200-kHz transducer, ± 2 cm vertical accuracy), a TSS 335B motion sensor that adjusted for roll/pitch of the vessel, and Max 4.3 Hydrographic Survey Software (Hypack, Inc., Middletown, CT) that accounted for water surface elevation changes across the site (Kulpa, 2006). Although discharge was essentially constant during bathymetric surveying (~34.3 m^3/s for the EDR and varied somewhere near ~158.6 m^3/s at the TBAR), the water surface profile was monitored through time using Insitu LevelTroll 500 pressure transducers (In-situ, Inc., Fort Collins, CO) positioned and surveyed for elevation along channel margins. In post-processing, a radial filter was applied to the bathymetric data to obtain a 0.61-m spacing between points. Quality assurance and quality control information beyond the scope of this summary can be retrieved from the contractor.

A permanent control network consisting of brass pins and masonry nails was established at each site with the Trimble RTK GPS. The control network enabled repeated channel margin, riffle crest, floodplain, and water surface elevation surveys using a Leica TPS 1200 robotic total station to supplement the bathymetric data. All total station surveying efforts were conducted using a grid approach with higher-density sampling where topographic complexity (slope breaks, drop-offs, and large boulders) necessitated more detail. Filtered bathymetric bed elevations were combined with total station data. Where the two datasets overlapped, geospatial (in a x,y,z coordinate system) comparisons showed consistency in the disparate measurement techniques and validated

the combination of the two approaches. A total of 15,705 and 47,765 points were mapped within the 2,588 m^3/s and 3,089 m^3/s channel margins (i.e. the lateral extent of inundation at each measured discharge) for the EDR and TBAR, respectively. Overall surveying density was 0.49 pts/m^2 at the TBAR and averaged 0.29 pts/m^2 in the floodplain and 1.07 pts/m^2 in the channel. Point density at the EDR was 0.94 pts/m^2 in the floodplain, 1.64 pts/m^2 in the channel, and 1.13 pts/m^2 overall.

4.1.2. Digital Elevation Model (Triangular Irregular Network)

DEMs represent topographic variation and, in this application, provide a surface for routing channel flow within a 2-D hydraulic model. In this study the DEM was created from the high resolution bathymetric and total station data acquired in the field. Total station and bathymetric survey data points were imported into ArcGIS 9.2 with 3D-Analyst for surface creation. Although a modified grid surveying technique was applied, a triangular irregular network (TIN) scheme was needed for interpolation to exploit the varied sampling density (Heil and Brych, 1978; Lee, 1991). Preliminary TIN surfaces were visually checked for topographic errors, compared to field reconnaissance notes, and modified with removal or addition of survey points to better characterize observed topography for both sites. Augmented and original data points were exported for mesh generation within the Surface-water Modeling System (SMS) graphical user interface.

4.2. Substrate Characterization and Analysis

Substrate conditions at each site were qualitatively and quantitatively characterized using photographs, maps, visual assessments, and pebble counts following the methods of Wolman (1954) and Kondolf (1992). Pebble counts consisted of approximately 100

randomly sampled bed particles from 9 m² (3 m x 3 m) sections in the active channel and surrounding floodplain at each site. Pebble count samples within the channel were limited to accessible areas and did not include the high velocity thalwegs at the TBAR and EDR. The intermediate axis size classes of sediment particles were determined using a sediment template and tallied to characterize size distributions for each sample. At the TBAR 87 pebble counts (avg. 120 pebbles per count) were completed in varying hydraulic conditions, while 5 counts (average of 123 particles) were conducted at the EDR in the summer of 2006. The small number of pebble counts at the EDR does not limit substrate characterization due to the homogenous nature of limited sediment deposits, which was validated by high-resolution aerial photographs and field notes. Despite initial qualitative differences observed between EDR and TBAR, the non-parametric Wilcoxon-Mann-Whitney Rank Sum test was used in Kaleidograph 4.0 (Synergy Software, Reading, PA) to determine if the D_{16}, D_{50}, D_{84}, and D_{90} size classes were statistically different. This method tests the hypothesis that two samples come from the same population. When reported alpha values are less than 0.05 this test suggests a statistically significant difference between two datasets.

4.3. Hydrodynamic Modeling

Hydraulic models like the Finite Element Surface Water Modeling System 3.1 (FESWMS) are frequently used to predict the spatial distribution of physical variables including velocity, depth, and shear forces along bridge structures, estuaries, coastlines, and habitat rehabilitation sites (Froehlich, 2002; Moir and Pasternack, 2008; Wang et al., 2004). FESWMS is a two-dimensional (depth averaged) hydrodynamic model best used

as a conceptual guide to depict river hydraulics. It assumes a horizontal water surface and negligible vertical velocity and acceleration components. The model was applied using the commercial graphical user interface Surface-Water Modeling System 9.2 (SMS) (Environmental Modeling Systems, Inc., South Jordan, UT), which greatly expedited the lengthy process of data pre-processing, modeling, visualization, and interpretation. Depth and velocity values at computational mesh nodes can be analyzed to predict potential spawning habitat and sediment entrainment, and therefore promote a conceptual understanding of ongoing hydrogeomorphic processes (Brown and Pasternack, 2008; Elkins et al., 2007; Ipson, 2006; MacWilliams et al., 2006; Moir and Pasternack, 2008; Pasternack et al., 2006).

4.3.1. Model Calculations

The FESWMS model was developed by the U.S Department of Transportation's Federal Highway Administration to solve steady and unsteady 2-D flow problems using the finite element method (FEM). The FEM is a numerical procedure for solving partial differential equations like those governing the equations of motion and mass continuity in river networks. This method breaks a modeled area into a mesh of triangular and quadrilateral elements, and then solves the set of applicable equations for nodes spaced along each element within the mesh. FESWMS solves the vertically integrated equations of motion in the x and y directions (equations 1 and 2 respectively) and mass continuity (3) for each node using the method of weighted residuals. Residuals are forced to vanish by numerically substituting values of dependent variables (depth and velocity) into the governing equations yielding a numerical approximation of depth and velocity that is

interpolated over the entire modeled mesh. For more information on how FESWMS obtains nodal solutions and interpolates depth and velocity values across the finite mesh see Froehlich (2002).

$$\frac{\partial}{\partial t}(HU)+\frac{\partial}{\partial x}(\beta_{uu}HUU)+\frac{\partial}{\partial y}(\beta_{uv}HUV)+gH\frac{\partial z_b}{\partial x}+\frac{1}{2}g\frac{\partial H^2}{\partial x}+\frac{1}{\rho}[\tau_x^b-\frac{\partial}{\partial x}(H\tau_{xx})-\frac{\partial}{\partial y}(H\tau_{xy})]=0 \quad \textbf{(1)}$$

$$\frac{\partial}{\partial t}(HV)+\frac{\partial}{\partial x}(\beta_{vu}HVU)+\frac{\partial}{\partial y}(\beta_{vv}HVV)+gH\frac{\partial z_b}{\partial y}+\frac{1}{2}g\frac{\partial H^2}{\partial y}+\frac{1}{\rho}[\tau_y^b-\frac{\partial}{\partial x}(H\tau_{yx})-\frac{\partial}{\partial y}(H\tau_{yy})]=0 \quad \textbf{(2)}$$

$$\frac{\partial H}{\partial t}+\frac{\partial}{\partial x}(HU)+\frac{\partial}{\partial y}(HV)=0 \quad \textbf{(3)}$$

H = water depth
U = depth-averaged velocity component in the horizontal x direction
V = depth-averaged velocity components in the horizontal y coordinate direction
z = the vertical direction
z_b = the bed elevation
u = the horizontal velocity in the x direction at a point along the vertical coordinate
v = the horizontal velocity in the y direction at a point along the vertical coordinate
$\beta_{uu},\beta_{uv},\beta_{vu},\beta_{vv}$ = momentum correction coefficients that account for the variation of velocity in the vertical direction
g = gravitational constant
ρ = water density (assumed constant)
τ^b_x,τ^b_y = bottom shear stresses acting in the x and y directions, respectively
$\tau_{xx},\tau_{xy},\tau_{yx},\tau_{yy}$ = shear stresses caused by turbulence where, for example, τ_{xy} is the shear stress acting in the x direction on a plane that is perpendicular to the y direction

4.3.2. Model Inputs

FESWMS uses field data to quantify input variables, boundary conditions, and model parameters. The four primary inputs are: 1) discharge, 2) downstream water surface elevation 3) channel margin boundaries 4) and a topographic boundary surface.

Discharge data for the Smartville and Deer Creek gages was collected from the California Data Exchange Center. Downstream water surface elevations were measured in the field for six discharges and combined with stream-gage data to compile a rating curve for each site. The only model run lacking measured downstream water surface data (the EDR 22.7 m^3/s) was approximated using the EDR rating curve. Channel margin locations were obtained from water surface edge surveys completed at specific discharges. For each model run a map delineating channel boundaries including upstream, downstream, and channel edges was constructed. In areas of greater hydraulic complexity (around boulders and channel margins) node spacing within the map was reduced to capture localized hydraulics where topographic survey resolution permitted. The map was used to generate a 2-D finite element mesh using the TIN paving scheme of SMS's mesh module. The resulting field of triangular and quadrilateral elements with equidistantly spaced nodes along their edges were checked for errors and corrected before topographic survey data were interpolated to mesh nodes. The resulting mesh yielded a complete lower boundary surface for routing channel flow.

Secondary inputs include user specified bed roughness and eddy viscosity parameters. Bed roughness was adjusted within SMS's mesh module interface to capture energy dissipation and resistance along the water/bed substrate boundary. As explained in Horritt (2006), roughness parameters for 2-D models can be broken into two components; one representing roughness below the scale of the DEM, and roughness associated with processes below the scale of the computational mesh. Extensive survey resolution was achieved in this study to reduce roughness effects of the former and Manning's *n* was used in model calculations to represent the latter. For practical

purposes Manning's *n* for each site was selected as follows. A roughness value for incised irregular bedrock channels similar to the EDR was absent from the literature and was at first estimated through expert opinion. During modeling an attempt was made to calibrate Manning's *n* by minimizing the deviations between modeled and observed water surface profiles. Five water surface surveys were conducted at the EDR, yet only two, the 33.7 m^3/s and 900.5 m^3/s discharge events, provided adequate reach length data for this analysis. Waves that surged against channel boundaries created water vapor that inhibited accurate total station measurements at higher discharges. Surveyed points were imported to the SMS scatter module where nearest node predictions of water surface elevation (±0.003 m) were extracted from the model. Overall, two Manning's *n* values were used at the EDR, one corresponding to discharges less than 710.7 m^3/s ($n = 0.032$) and one for discharges equal to and exceeding 710.7 m^3/s ($n = 0.038$). Although studies suggest that roughness is spatially complex and stage dependent, a constant Manning's coefficient was used for all model runs at the EDR.

For the TBAR model runs below 267.8 m^3/s a Manning's coefficient of 0.030 was used to capture channel roughness. At discharges exceeding this value, where willow patches along channel margins were inundated, an attempt to incorporate the increased roughness was made following the methods of Freeman (2000). A roughness value of 0.052 was attributed to elements that coincided with inundated willow patches at these increased discharges. The roughness coefficient used in model calculations for the TBAR is consistent with those reported values for cobble and gravel streams (Chow, 1959).

Eddy viscosity, a parameter used to capture transverse mixing associated with

turbulent flow, is a sensitive variable in 2-D model applications in bedrock channels (Miller and Cluer, 1998). FESWMS uses the Boussinesq eddy viscosity method which assumes that turbulent stress terms in the governing equations are proportional to local velocity gradients (Miller and Cluer, 1998). This treatment of turbulence closure is included in the system of model equations explained above and allows a more representative prediction of transverse velocity gradients than methods which hold E constant. In FESWMS, node value eddy viscosities are calculated using equations 4 and 5 where u* is shear velocity, Cd is a coefficient of drag represented by equation 6, and E_o is a minimized empirical constant of 0.033 $m^2 s^{-1}$. Eddy viscosities set too high reduce transverse mixing and cause models to underestimate turbulent eddy features, lateral velocity variability, and mid channel velocity, while extremely low eddy viscosities promote model instability.

$$E = 0.6H \cdot u* + E_o \quad \textbf{(4)}$$

$$u* = U\sqrt{Cd} \quad \textbf{(5)}$$

$$Cd = \frac{9.81n^2}{H^{1/3}} \quad \textbf{(6)}$$

4.3.3. Model Performance

Although the FESWMS model has been thoroughly validated on the gravel-bed Mokelumne (Elkins et al., 2007; Wheaton et al., 2004a) and Trinity (Brown and Pasternack, 2008) Rivers, an investigation of its relevance along the Yuba River was still warranted for this study. Recently, Moir and Pasternack (2008) reported a FESWMS modeling and validation study at the TBAR using data from 2004-2005, prior to a large

flood that yielded the morphology investigated in this study. For this new morphology, depth and velocity were recorded at three cross sections during the 18.4, 21.2, and 31.2 m^3/s low flow events at the TBAR and compared against modeled predictions by surveying (±2cm) the locations of depth and velocity measurements with the Leica 1200 system described above. Velocity was measured at 60% of water column depth using a depth setting rod and Marsh McBirney electromagnetic flow meter averaged for 30 seconds at 30 Hz to approximate average column velocity. The coordinates of depth and velocity measurements were imported to the SMS mesh where the nearest depth and velocity node predictions were used to test the model. A best fit curve was applied to modeled and measured datasets to ascertain the predictive capabilities of the model across the channel.

Performance of the model at the EDR was evaluated by plotting the field measured and final modeled water surface profiles across the site for the 33.7, 271.3, and 900.5 m^3/s discharge events. For each event, the most upstream water surface elevation point was used as the datum. Although a cross-sectional comparison of depth and velocity similar to the TBAR would be a more robust test of model capability at the EDR, logistical and field constraints prohibited the use of this method. For example, much of the EDR cannot be waded and precludes any direct measurement of depth and velocity at a cross section. Even access by boat is a difficult task to achieve and requires a portage of a shallow rapid downstream of the EDR.

4.4. Shields stress Calculations

Shields stress is a common dimensionless parameter used to predict sediment entrainment in gravel-bed rivers (Elkins et al., 2007; Lisle et al., 2000). It is the ratio of shear stress (τ) to the submerged weight of a sediment particle of a specific grain size. To get an approximation of Shields stress the drag coefficient method of calculating shear stress was employed, where shear stress is equal to the product of water density (ρ_w), a drag coefficient (Cd), and velocity squared **(**Eqn. 7**)**. Water density was assumed constant and velocity values were exported from model predictions. As outlined above, the drag coefficient (Cd) was approximated as a function of Manning's *n* and channel depth; the former fixed in each model scenario and the latter exported along with velocity values for each node in the mesh. Overall, depth and velocity predictions were used to calculate drag coefficients **(Eqn. 6)**, shear stress **(Eqn. 7)**, and Shields stress **(Eqn. 8)** at each mesh node where γ_s and γ_w are the specific weight of sediment and water, respectively, and D_{50} is the median sediment particle size in mm. Shields stress values were calculated within SMS in a stepwise fashion and adjusted by a factor of 0.51 to account for lower real-world near bed velocities (MacWilliams et al., 2006; Pasternack et al., 2006).

$$\tau = \rho_w C d U^2 \qquad \textbf{(7)}$$

$$\tau^* = \frac{\tau}{(\gamma_s - \gamma_w) D_{50}} \qquad \textbf{(8)}$$

Shields stress values of $\tau^* < 0.01$, $0.01 < \tau^* < 0.03$, $0.03 < \tau^* < 0.06$, and $\tau^* > 0.06$ correspond to no transport, intermittent transport, partial transport, and full transport

regimes, respectively, as defined by (Lisle et al., 2000). These ranges helped to account for uncertainty in depth and velocity predictions. The Shields stress classes adopted here provide a conceptual understanding of sediment transport, but it is important to appreciate that transport is a probabilistic phenomenon and not governed by strict thresholds. For example, Paintal (1971) showed that even though shear stress values are below the critical value required for "insipient motion", some form of transport is likely to occur, which corresponds to the intermittent transport class used in this study. Overall the qualitative definitions of the Shields stress classes are as follows: no transport corresponds to a stable bed, intermittent transport corresponds to minimal transport associated with turbulent bursts, partial transport suggests that particle entrainment will occur for a specific sediment size class if it is in relative abundance on the bed (compared to other particle sizes), and full transport suggests a carpet of sediment moving along the boundary.

The method of Shields stress calculation outlined above makes explicit assumptions about the relationship between Shields stress and various physical variables. For instance, τ^* is proportional to both velocity and Manning's n to the second power, suggesting that Shields stress increases with channel roughness and velocity in a nonlinear fashion. Model predicted Shields stress values were exported from SMS and spatially analyzed within ArcGis 9.2.

4.5. Habitat Modeling

FESWMS provides depth and average velocity predictions central for describing potential spawning habitat within a rehabilitation site. Habitat suitability curves (HSCs),

polynomial regressions between key spawning variables (e.g., depth, velocity) were used to relate predicted hydraulic variables and available physical habitat. For this study a depth and velocity HSC developed for the Mokelumne river fall run Chinook salmon was used to predict physical spawning habitat quality from model solutions (CDFG, 1991). Various field studies have shown that habitat suitability curves vary not only by species, but may also vary by watershed, fish size, and specific physical conditions including temperature and hyporheic upwelling (Giest and Dauble, 1998). Thus, the Mokelumne River HSCs were tested and validated for use on the Yuba River as described below. Predicted node depths and velocities were exported and entered into the Mokelumne River depth and velocity HSCs, which produced a measure of habitat quality for each node between 0 (no habitat) and 1 (highest quality). The contribution of depth and velocity to overall habitat suitability were evenly weighted and used to create an index defined as the geometric mean of the two independent depth and velocity functions **(Eqn. 9)**. V(x) and D(y) represent the velocity and depth suitability functions (HSCs) formulated for the Mokelumne River fall run Chinook. The combined habitat suitability metric, denoted the geometric habitat suitability index (GHSI), was calculated at each node and interpolated over the modeled area giving a spatial distribution of predicted habitat that was compared across sites. GHSI values were broken into four classes that qualitatively represent poor (0.0-0.2), fair (0.2-0.4), good (0.4-0.6), and excellent (0.6-1.0) habitat.

$$GHSI = \sqrt{V(x) \bullet D(y)} \qquad \textbf{(9)}$$

4.5.1. Habitat Model Performance

To evaluate the performance of Mokelumne River HSCs, salmon redd locations were surveyed on fifteen days between September 7th and November 15th 2005 at the TBAR and overlaid onto the model predicted GHSI mesh. Observed redds were divided into two groups based on the dominant measured discharge. The first represented redds observed while flows were approximately 22 m^3/s and the second represented redds observed at 34 m^3/s. Redds were identified in the channel by expert observers that keyed in on disturbed sediment patches, pit and tailspill morphology, and direct observations of spawning salmon. The location of each redd pit was surveyed with the Leica 1200 system described above while weighted tags were placed adjacent to each pit to reduce repetitive sampling. Tags that were buried or moved suggested a new spawning event occurred and the redd structure was surveyed again. Overall, survey procedures provided ± 0.02 m horizontal accuracy for comparing locations of redds against model predicted GHSI values.

An electivity index was constructed to test the Mokelumne River HSC's ability to capture observed habitat preferences. First, a raster data set of model predicted GHSI values in ArcGIS 9.2 for the 21.2 m^3/s model run was created. The total channel area in each GHSI class was exported using the zonal statistics tool in spatial analyst and raster values (GHSI) at redd locations were extracted. The percent of channel area and observed redds within each GHSI class was calculated and plotted. Following the work of Ivlev (1961), the electivity index method was used, where E is the ratio of the proportion of redds observed to the proportion of channel area within a GHSI class **(Eqn. 10)**. Values less than one (<1) suggest fish use a specific habitat less than its availability

(avoidance) while values greater than one (>1) suggest a particular habitat class is used more often than its availability (preference). The electivity indices for each of the four habitat suitability classes were calculated and analyzed for preference and avoidance phenomena.

$$E = \frac{\%Redds_{GHSI}}{\%Habitat_{GHSI}} \quad \textbf{(10)}$$

4.6. Imagery

Historical photographs and aerial imagery are fundamental tools for characterizing channel form, sediment deposits, and reconstructing site morphogenesis. Research at the turn of the century (ca. 1909) by G.K. Gilbert and USACE photographs of the LYR between the current locations of Englebright and Daguerre Dams were obtained from the USGS (2006) photographic library and government agencies respectively. Aerial images were available from James (2007) and Terraserver® (2007) for 1937, 1947, 1952, 1958, 1984, 1986, 1991, 1996, 2002, 2004, 2005, and 2006. Although aerial imagery was not used for detailed analysis in this study, it provided a depiction of system evolution.

4.7. Sediment Transport Analysis

A vital component of restoration efforts aimed at ameliorating sediment discontinuity below dams is an estimation of sediment transport to the project reach. Although current delivery to the EDR is negligible, two broad quantitative estimates of sediment transport within the LYR were made based on (1) swath bathymetry and sediment core data acquired by Snyder (2004), and (2) repetitive topographic surveys of the TBAR as described above.

Using the conservative variable layer method of calculation reported in Snyder (2004), percent gravel in sampled cores was multiplied by total mass of sediment for each layer area and summed for the entire lake deposit. The resulting number represents the total mass of gravel locked behind Englebright. Total volume of gravel detained by Englebright was estimated by dividing total gravel mass with an average bulk density of 1.65 kg/m³. An assessment of average annual load was made by equally distributing the total volume of gravel over the 61 years since Englebright was completed, providing an average annual load that would have reached the EDR without the dam upstream.

A secondary, event specific, approximation of transport for the LYR was conducted through DEM differencing methods by surveying bed topography at the TBAR before and after the December 2005 3,089 m³/s (24-yr) flood event. This method quantifies changes in the storage component of a sediment budget, an overall accounting of inputs, outputs, and sediment storage in a channel. Topographic points from the pre and post flood survey were used to create separate DEMs using the TIN interpolation method described above. DEMs were rasterized to cells of 0.023 m² within ArcGIS 9.2 3D Analyst and the 2005 raster was subtracted from the 2006. This produced a new raster representing elevation deviations attributable to the flood. To account for bed elevation variability and sub resolution noise, elevation deviations of ± 0.051 m were filtered out and not considered in the differencing analysis. Volumetric estimations of transport at the site were produced by multiplying elevation deviations by the appropriate cell size.

5. HYPOTHESIS TESTING

Empirically and numerically generated data streams were used to reject or accept the hypotheses presented in **Table 1**. The general testing methodology for each hypothesis is presented below and the relevancy to GA efficacy at the EDR will be discussed.

5.1. Bed Material

H_1: *Sediment characteristics at the EDR and TBAR are comparable and suitable for spawning.*

A sediment characterization, represented by empirically derived diameter statistics and observations of particle shape (roundness, sharpness), was used to determine if sediment conditions were within the known preference range (12-80 mm) of Chinook salmon at the EDR (Kondolf, 1993). If sediment particles at the EDR are substantially coarser or more angular than TBAR sediments or if a significantly smaller fraction of particles fall within the limits of Chinook preference curves, then hypothesis H_1 will be rejected. The former was tested by comparing the D_{16}, D_{50}, D_{84}, and D_{90} size classes at each site using the Wilcoxon-Mann-Whitney Rank Sum test mentioned above with an alpha value of 0.05. A qualitative test of the latter was completed by comparing particle roundness through field observations and imagery of the two sites.

5.2. Hydraulics

H_2: *Flow convergence routing will enable the injection of small doses of gravel to produce alluvial geomorphic features (riffles, pools, glides) that accentuate the existing pattern of topographic highs and lows at the EDR and TBAR study sites.*

Model predicted velocity fields for the six comparable discharge events were analyzed for flow convergence effects. The presence of a velocity reversal, associated with confinements upstream of pools at high discharges would suggest that deposition of augmented gravels will occur downstream of pools on topographical highs (sills) and maintain site morphology. The absence of a velocity reversal at either site would suggest that alluvial deposition on bedrock sills and riffle-habitat formation is not likely to occur. In that case, the injection of small doses of gravel would only serve to fill in pools or accumulate along channel margins. If a velocity reversal is not observed at the EDR, H_2 will be rejected.

5.3. Geomorphology

H_3: *Injected gravels at the EDR will be stable during spawning flows.*

H_4: *Injected gravels at the EDR will be stable during a 271.3 m³/s discharge (2-year event).*

H_5: *Injected gravels at the EDR will be stable during a 900.5 m³/s discharge (~5-year event).*

H_6: *Injected gravels at the EDR will be stable during a 2588.2 m³/s discharge (~24-year event).*

To determine the likelihood of gravel mobilization the proportion of wetted channel within each Shields stress class was calculated to test hypotheses H_3-H_6. Each hypothesis will be rejected if a significant proportion of the channel (10%) registers in the full transport regime.

H_7: *GA will aggrade the EDR and produce extensive cross channel habitat that is susceptible to scour.*

Historical images depicting site morphogenesis, an estimation of sediment transport, and Shields stress in the spawning channel of the EDR were used to infer the likelihood of scour and deposition patterns. H_7 will be rejected if the underlying response of the system is to rapidly evacuate injected gravels and produce heterogeneous depositional patterns.

5.4. Habitat

H_8: *Historically, the EDR supplied ample spawning habitat for Chinook salmon.*

Historical images, observations of spawning behavior at the EDR, and a literature review provided a means for testing H_8. Overall, H_8 will be rejected if historical evidence suggests that salmon spawning at the EDR was limited in spatial extent and frequency.

H_9: *Current spawning habitat at the EDR and TBAR is not limited.*

The percentage of channel in the poor, fair, good, and excellent quality habitat was calculated with HSCs and ArcGIS 9.2 for the 33.7 m^3/s EDR and 34.6 m^3/s TBAR and compared. If the proportion of channel in the medium and high quality class is below 5% of the wetted channel area H_9 will be rejected.

6. RESULTS

6.1. Topography

DEMs of the two project sites are presented in **Fig. 7** to highlight topographical diversity and facilitate general morphologic comparisons. The EDR exhibits a pool/run/pool sequence with near vertical canyon walls confining the single channel on the south and inhibiting lateral channel migration. To the north, a 20 m wide by 40 m long deposit of blast rock bolsters the channel edge before adjacent hillsides impinge the irregular elevated floodplain. Topographic variability of the bed is pronounced, influenced by the character (slope, curvature) of surrounding hill-slopes, and controls hydraulic variables within the channel. For example, hillsides on the northern edge of EDR are more gradual than on the south, resulting in shallower depths for a given discharge along the northern channel edge. Further topographic control is evident between the head and tail of the run where two bedrock features jut into the channel from the southern hillside forming shallow shelves (aka "sills"). During spawning flows (22-34 m^3/s) the channel is widest in the Narrows pool (~40 m), constricts through the run (~20 m), and expands slightly below the 2^{nd} bedrock feature (~28 m) before reaching the Narrows I powerhouse 600 m downstream of Englebright Dam. At a discharge of 2588.2 m^3/s, channel width is uniform throughout the 135 m reach and averages ~64 m.

The TBAR exhibits gradual slopes along channel margins and is less influenced and constrained by surrounding hillsides than the EDR. A highly connected floodplain and adequate sediment supply allows significant channel migration during extreme events along the pool/island/riffle sequence. Two topographic lows in the middle of the site represent the main and highly complex side channel that merge downstream of a depositional mid-channel island bordering the main riffle on the north. During spawning flows the main channel constricts from ~100 m at the head of the island to ~ 45 m at the

riffle crest before transitioning to a narrow (~22 m) thalweg that cuts across the tail of the island. Topographic variation at the subunit scale (10^0) is extensive near two bedrock outcrops that promote pool formation downstream and along island margins. This topographic heterogeneity provides an array of physical habitat types including pools, riffles, recirculating eddies, shallow margin zones, and cut banks for differing life stages of salmonids (Moir and Pasternack, 2008).

6.2. Roughness Calibration

Initial efforts were made to calibrate the model by adjusting Manning's *n* values to attain convergence between predicted and observed water surface profiles. **Table 3** provides the results of calibration using the 75 and 20 field measured water surface profile points acquired in the field for the 33.7 m^3/s and 900.5 m^3/s discharges, respectively. To avoid closure errors, eddy viscosity values were altered to attain model convergence in accordance with Rameshwaran (2003) who found that eddy viscosity had little effect on channel roughness calibration. Overall, changing Manning's *n* from 0.022 to 0.040 causes an average absolute profile deviation of 0.007 m or 0.41 % of mean channel depth for the 33.7 m^3/s event. Calibration efforts altered average absolute errors for the 900.5 m^3/s model run by 0.08 m or 0.43% of channel depth.

6.3. Model Performance

6.3.1. TBAR Hydraulics

Model predictions and field measurements of depth and velocity for 83 points along three cross sections at the TBAR are presented in **Fig. 8** for validation purposes. At cross

section 1 with a discharge of 18.40 m³/s, the average absolute depth and velocity errors were 0.05 m and 0.04 m/s. At a discharge of 21.15 m³/s the model under predicted depth for the entire length of cross section 2 and over-predicted velocity along the northern side of the channel with average absolute errors in depth and velocity of 0.08 m and 0.04 m/s. At a discharge of 31.18 m³/s at cross section 3, absolute errors in modeled versus measured predictions were 0.03 m and 0.05 m/s for depth and velocity. Despite these inaccuracies, raw comparisons of all modeled and observed values provided a coefficient of determination of 0.929 and 0.768 for depth and velocity, respectively. Overall, depth and velocity predictions for each cross section have a mean error of ±10% for depth and ±22 % for velocity.

6.3.2. EDR Water Surface Profiles

Surveyed water surface elevation data along the channel edges provided a means to assess model predictions of water surface elevations for the 37.7, 271.3, and 900.5 m³/s discharges at the EDR. For the 37.7 m³/s event, a channel roughness coefficient of n = 0.032 caused the model to over predict water surface elevation through the majority of the site with an average absolute error of 1.1 % of channel depth **(Fig. 9)**. Although modeled water surface elevation deviated from the measured locations, the coefficient of determination for raw differences was 0.89. The model predicted water surface elevation for the 271.3 m³/s discharge was less accurate and had an error of 6% of average channel depth. Overall, there was a parallel between the two sets with the model consistently over-predicting water surface elevation in a downstream direction. The coefficient of determination between modeled and measured data points for the 271.3 m³/s discharge

was 0.76 using a Manning's *n* of 0.032. At the highest analyzed discharge of 900.5 m^3/s and using a Manning's roughness value of 0.038, an error of 1.57% of average channel depth (0.08 m) was observed with a coefficient of determination registering at 0.89.

6.3.3. Habitat Suitability Curve Performance

Two hundred and forty redds were mapped at the TBAR during the two spawning discharges. Model predicted GHSI values and the 110 observed redds for the 21.2 m^3/s event are presented in **Fig. 10**. Predictions for the higher spawning flow are similar but left out for sake of brevity. Redds and model predicted good and excellent habitat classes are clustered around the island head and downstream of the island tail. Some redds and high quality habitat areas are located in very narrow zones along the side channel. The results of the electivity analysis, including the percent of channel area and percent of observed redds in each of the habitat suitability bins, are presented in **Fig. 11**. Electivity values for the poor, fair, good and excellent habitat suitability classes were 0.16, 0.22, 1.61, and 3.56, respectively. Overall, poor and fair quality habitat covered ~ 67 % of the channel area while good and excellent habitat amount to ~32 % of the channel.

6.4. Bed Material

6.4.1. Hypothesis H_1

Sediment size distributions based on five pooled bed samples at EDR validated field observations on the coarseness of the heavily altered channel **(Fig. 12)**. Average D_{16}, D_{50}, D_{84}, and D_{90} values were 50.0, 144.3, 327.9, and 382.5 mm for the EDR, respectively. Obvious intra-site variation was absent although a limited sample size may

have obscured patterns that visual assessments had indicated. For example clast size appears to increase moving away from the channel. Overall only ~25 % of sampled particles at the EDR were within the size limits of spawning gravels reported in the literature and all were highly angular.

At the TBAR 87 pebble counts were pooled to obtain reach average values; cumulative frequency plots depict a site dominated by cobble and gravel with computed D_{16}, D_{50}, D_{84}, and D_{90} values of 36.7, 74.2, 138.9, and 162.3 mm, respectively **(Fig. 12)**. General patterns of intra-site variation were evident and controlled by local hydraulic conditions. Overall a significant portion (~50%) of the sampled area at the TBAR contained gravels of appropriate size and character for Chinook salmon. The alpha values for the Wilcoxon-Mann-Whitney rank sum test were 0.057, 0.00054, 0.00018, and 0.00018 when comparing the D_{16}, D_{50}, D_{84}, and D_{90} size classes at the EDR and TBAR.

6.5. Hydraulics

6.5.1. Hypothesis H_2

The spatial distribution of depth and velocity for the six EDR modeled discharges are presented in **Fig. 13 & 14** respectively and are dominated by local bedrock topography. For all model runs depth is greatest in the Narrows II pool afterbay. There was a general longitudinal pattern of depth decreasing downstream of the Narrows pool, staying consistent in the run section, and increasing again downstream of the second bedrock constriction **(Fig. 13)**. At the two modeled spawning flows, depth at the exit of the Narrows pool and throughout the channel is consistently >1 m except along channel margins. A maximum velocity of 1.5 m/s occurred near two bedrock features that

laterally constricted and accelerated flow **(Fig. 14A)**. For the lowest two discharges velocity decreased between the bedrock features before accelerating over the second shelf and into the lower pool **(Fig. 14 A & B)**. For discharges above 33.7 m^3/s deceleration in the run was less pronounced and the location of maximum velocity swelled to incorporate the entire mid-section of the modeled reach **(Fig. 14D, E, & F)**. A maximum velocity of 6 m/s was predicted in the 2588.2 m^3 discharge scenario where velocity in the entire run was above 5 m/s. The location of maximum velocity showed little variation across discharges and coincided with the two constriction points denoted in the DEM.

The spatial distribution of depth and velocity at the TBAR for all modeled discharges is presented in **Figure 15** and **16** respectively. Depth was greatest in the main channel thalweg downstream of the riffle crest and along the side channel in the forced pool complex. During spawning flows at the TBAR, depths across the riffle ranged from 0-1 m. Velocity at the TBAR was more variable than the EDR for the low (21.2 m^3/s) spawning flow **(Fig. 16A)**. Maximum velocity (~3 m/s) occurred downstream of the main riffle crest where lateral convergence accelerated flow and directed it through the narrow thalweg. Spatial patterns of velocity were similar for the 34.6 m^3/s discharge event **(Fig. 16B)**, but as discharge increased to 267.8 m^3/s **(Fig. 16C)**, the model predicted an increase and shift in maximum velocity (4 m/s) to the run 60 m downstream of the island tail. Interestingly, more than doubling the discharge to 655.3 m^3/s had little effect on maximum velocity, yet the region that exhibited > 3 m/s increased dramatically and covered ~75% of the site **(Fig. 16D)**. For discharges exceeding 998.4 m^3/s, velocity increased towards the channel center, and reached a maximum value of 4.5 m/s in the

upstream pool and over the island tail for the 3089.1 m³/s event. Overall, velocity variation was dampened at higher discharges and a velocity reversal was detected.

6.6. Geomorphology

6.6.1. Hypotheses H_3-H_6

The spatial distribution of Shields stress was calculated using the D_{50} of spawning sized sediments for the six EDR flows **(Fig. 17)**. Intermittent transport was predicted from the run entrance throughout the entire mid-channel for the 271.3 m³/s EDR discharge **(Fig. 17C)**. A localized patch of partial transport was also predicted in the center of the run between the two topographic features constricting the channel. Except for margin areas, the entire channel was under intermittent transport at a discharge of 710.7 m³/s while partial transport extended mid-channel from the run entrance through the downstream boundary **(Fig. 17D)**. Between the 710.7 m³/s and 900.5 m³/s discharge events, full transport in the run increased by 7% of channel area and partial transport expanded laterally and upstream into the Narrows II pool exit **(Fig. 17D & E)**. At 2588.2 m³/s, the entire mid-channel section of the EDR was under full transport with localized areas within the run registering in the highest of Shield stress values **(Fig. 17F)**.

For the 900.5 m³/s and 2588.2 m³/s events, the model predicted Shields stress values corresponding to "full transport" in 15% and 54% of the wetted channel area, respectively **(Fig. 18)**. Significant full transport was not predicted for the spawning (22.7 and 33.7 m³/s) flow or 2-year event (271.3 m³/s) discharge. Overall, Shields stress for all modeled discharges was at a maximum in the run between the two topographic boundary controls and minimized along channel margins.

Unlike the EDR, intermittent transport was predicted at the TBAR below the riffle crest, through the narrow thalweg, and in the run section downstream of the island for the two modeled spawning flows **(Fig. 19A & B)**. At a discharge of 267.8 m^3/s, intermittent transport was predicted throughout the TBAR with a section of partial transport near the downstream boundary corresponding to the velocity increase in that area **(Fig. 19C)**. Aside from a small zone of full transport associated with increased element roughness in the willow margin, significant full transport was not predicted in the channel until discharge exceeded 998.4 m^3/s **(Fig. 19D & E)**. During the 3089 m^3/s flood event at the TBAR Shields stress values above 0.1 are predicted throughout the channel center, and peak in the pool upstream of the main riffle and at the valley constriction evident in the DEM. Overall, approximately 1% and 46% of the channel were in the full transport regime for 998.4 m^3/s and 3089 m^3/s respectively at the TBAR.

6.6.2. Hypothesis H_7

Numerous historical photos helped characterize the Yuba River around the EDR and provided a conceptual understanding of ongoing geomorphic processes and system evolution. An image taken 0.4 km upstream of the EDR by G.K. Gilbert in 1909 facing upstream is the earliest available high quality photo of the Yuba river near the project site **(Fig. 20)**. Although the picture was taken 400 meters upstream of the EDR, the morphology pictured is representative of conditions throughout the narrow bedrock lined reach at that time. Steep canyon walls border the channel on both sides and extensive bedrock control is evident. Interestingly, a deposit of hydraulic mining debris remains in the channel forming a small riffle complex on river left (right in picture). Gravel deposits

are also present behind protruding bedrock features upstream and along channel margins. Overall, the channel is confined and dominated by angular resistant bedrock features that protrude into the channel and allow deposition of cobble and gravel size material in their lee.

During the construction of Englebright Dam substrate conditions at the EDR were highly manipulated. Dynamite was used to raze weathered rock from surrounding hillsides while steam shovels and dump trucks moved large quantities of rubble around the site **(Fig. 21)**. Angular blast rock was built up on river left and formed a large terrace bordering the southern channel margin. The blast rock terrace has since been removed by numerous flood events and transported downstream. The volume of rock removed from surrounding hillsides is unknown yet its effect on channel substrate is documented by field mapping of continuous blast rock deposits from the EDR to downstream of Deer Creek.

A 1909 image provided by G.K. Gilbert 0.5 km downstream of the EDR overlooking the Deer Creek confluence depicts a bedrock channel inundated with large quantities of hydraulic mining debris **(Fig. 22A)**. The bar on river right extends past the Deer creek confluence and bedrock features within the channel are completely covered. A recent photo of the Deer creek confluence from about the same location clearly shows the amount of sediment removed in the 98 years since Gilbert's photo through incision processes **(Fig. 22B)**. Cobbles and hydraulic mine debris are virtually absent, and the large bar on river right has been replaced with resistant blast rock washed down from the construction of Englebright. The lateral bar on river right no longer extends beyond the

Deer Creek confluence and all remaining coarse hydraulic mine sediments are greater than 30 m above the low flow water surface elevation.

As reported by Snyder (2003), over 25% of Englebright Reservoir's initial capacity has be filled with ~26 x 10^6 metric tons of sediment consisting of silt, sand, gravel, and organic material. Of this, the approximate mass of gravel retained by Englebright is ~ 4.73 x 10^5 metric tons. With an assumed bulk density of 1.65 kg/m³, this is equivalent to a volume of 2.86 x 10^5 m³ of gravel. Distributing the total mass and volume over the 61 years since Englebright was completed produces an estimated annual load of 77520 metric tons/yr or 47124 m³/yr of gravel that would have entered the EDR.

The DEM differencing analysis at the TBAR provided the spatial distribution of cut and fill attributable to the December 2005 24-year flood event, and an approximate estimate of transport **(Fig. 23)**. A net loss of 19,984 m³ cubic meters occurred at the site with 30,057 m³ and 10,073 m³ of scour and deposition respectively. Topography was completely reworked and channel morphology changed dramatically. The location of the island moved downstream towards river left and a new side channel formed along the southern valley margin. Maximum scour and fill within the reach was ~ 2.4 m and 2.25 m respectively with a negligible change in average channel elevation. Overall, the volume of sediment removed from the TBAR represents a lower bound estimate of transport, as much more material could have moved through the site during the event and subsequently replaced by sediments from upstream.

Model predicted Shields stress values for the 2-yr, 5-yr, and 24-yr events were overlain on the area of channel inundated at spawning flows for the EDR. The resulting map represents the spatial distribution of probable scour and deposition within the

spawning channel area for the modeled events at the EDR **(Fig. 24)**. For a typical 2-year event partial transport will occur in the narrowest section of the spawning channel but as the channel expands laterally moving downstream, velocity decreases and Shields stress was reduced **(Fig. 24A)**. During a 5-yr event, significant full transport on the along the northern channel boundary was predicted with most of the spawning channel in partial transport **(Fig. 24B)**. During the 24-year event, full transport dominated the spawning channel **(Fig. 24C)**. Results show that for all discharges Shields stress was lowest along channel margins and specifically downstream of major bedrock/topographic features that protrude into the channel. For all discharges a relatively stable environment occurs along the southern side of the channel at the tail of the Narrows pool afterbay.

6.7. Habitat

6.7.1. Hypotheses H_8

Gilbert's 1909 image **(Fig. 20)** also provides some information about the character of spawning habitat that may have formed in this active supply limited channel. The small riffle present in the foreground and channel margin/boulder deposits of sediment in the background show that despite the transport dominated regime, gravel and cobble-sized material (presumably hydraulic mining debris) was deposited and may have provided suitable sediments for spawning salmonids. It is difficult to predict, but sediment input to the channel prior to hydraulic mining may not have filled the channel to the same extent, however some deposition of suitable gravels likely occurred. Regardless, the image clearly shows that significant lateral bars and riffle features do not exist at a time of

extreme sediment supply and that the spatial pattern of deposition in the channel is not continuous.

Field observations and historical accounts provide meaningful clues about the magnitude and extent of historical spawning habitat at the EDR. For example, multiple pairs of salmon were observed spawning near the Narrows I powerhouse throughout the 1970s and early 1980s (Mullican, 2007). Although the location of the observed spawning activity is roughly 200 m downstream of the EDR, substrate conditions were likely comparable. On two other occasions, (October 10th 2005 and September 25th 2007), the author observed large (~800 mm) female salmon "testing" sediments along channel margins at EDR by turning horizontal in the water column and attempting to dislodge particles from the bed through body flexing. In both cases, female salmon were unable to mobilize sediments and successful spawning was not observed.

6.7.2. Hypotheses H_9

Medium and high quality habitat predictions at the EDR, based solely on hydraulic variables, were limited to small (< 0.5 m²) strips along channel edges while habitat associated with pool exits/riffle entrances was nonexistent. Overall, 87%, 10%, 2%, and <1% of the wetted channel was in the poor, fair, good, and excellent quality habitat classes at the EDR for the 33.7 m³/s spawning flow **(Fig. 25A)**. At a discharge of 21.2 m³/s FESWMS predicted extensive medium and high quality habitat at the pool exit/riffle entrance and forced pool/riffle complex adjacent the to the island tail at the TBAR **(Fig. 10)**. Results for the higher (~34.6 m³/s) discharge were similar but left out for sake of brevity. Localized areas of margin habitat exist, and predictions are substantiated by

observed redds within the side channel. The proportion of channel in the poor, fair, good, and excellent quality habitat were approximately 36%, 29%, 18%, and 15% respectively at the TBAR.

A decomposition of the geometric habitat suitability index into its component depth and velocity functions within the modeled mesh provided an areal distribution of depth and velocity habitat suitability for the EDR 33.7 m^3/s spawning flow **(Fig. 25B &C)**. While velocity is suitable throughout the channel center, depth is adequate only along channel edges. At the pool exit, the most frequently utilized location of spawning activity in the LYR, depths are greater than those preferred by Chinook salmon (given the HSCs employed) and averaged between 1 and 2 m. Although not provided, habitat predictions for the 22.6 m^3/s EDR spawning flow provide the same spatial patterns of habitat.

7. DISCUSSION

For organizational purposes the following section has been separated into two parts. The first three divisions (7.1-7.3) are directed towards methodological issues such as roughness calibration, model behavior (hydraulics) and habitat validation. The second part (divisions 7.4-7.7) discusses results directly related to the stated hypotheses.

7.1. EDR Roughness

Roughness calibration results at the EDR suggest that in bedrock channels the 2-D model FESWMS was rather insensitive to Manning's *n* when it comes to matching observed and modeled modeled water surface profiles. Changing Manning's *n* from

0.022 to 0.040 in the 33.7 m^3/s run altered average absolute errors by only 0.41% of channel depth **(Table 3)**. Ghanem (1996) found similar results after calibrating a 2-D model in which changing roughness by 100% caused an 8% increase in channel depth.

Model insensitivity in the roughness parameterization scheme can be attributed to the scale of dominant roughness elements in the channel and their accurate representation in the DEM. The DEM in this study consisted of high density (1.44 points/m^2) survey data that resolved the dominant roughness features like lateral bedrock constrictions, resistant inundated boulder clusters, and overall bed-form irregularities. Previous 2-D model applications have shown significant model sensitivity to the representation of topographic complexity. Detailed survey procedures increased the resolution of roughness characterization and implicitly incorporated it into the surface over which flow was routed. In effect, this increased the overall proportion of roughness accounted for in model simulations. Furthermore, unlike gravel-bed streams where roughness associated with individual grain diameters may be quite important, channel roughness in bedrock channels is dominated by larger scale features best characterized through the direct intensive surveying methods employed here. Overall, the insensitivity of water surface deviations to Manning's *n* suggests that the topographic characterization of the EDR adequately describes a high proportion of roughness elements in the channel.

All three of the modeled water profiles at the EDR followed the general form of measured water surface elevation and are comparable to errors reported in other studies. For instance, the maximum observed error of 6% of channel depth for the 271.3 m^3/s event is within the 0.11 m and 0.23 m range (5.1%-15.4% of channel depth respectively) reported by Miller (1998). Both the 33.7 m^3/s and 900.3 m^3/s event registered errors

smaller than the lower limit of 0.11 m referenced above. The largest error for the 33.7 m^3/s occurs at the location of a channel protruding bedrock outcrop 60 m from the upstream datum and was likely caused by the model's inability to capture vertical accelerations that result from the constriction and associated vertical momentum flux that occurred at this location. Unlike Miller (1998), a correlation between water surface errors and discharge was not observed, further suggesting the adequacy of the constructed DEM. Overall, a general agreement is observed between model predicted and measured water surface profiles with errors equal to or below previous studies in bedrock channels. Further investigation into the ability of FESWMS to capture spatial patterns of velocity and depth is warranted.

7.2. TBAR Hydraulics

The three cross-sectional comparisons of measured and modeled depth and velocity at the TBAR validate FESWMS's ability capture channel hydraulics in gravel bed channels. As reported in Moir and Pasternack (2008), the model accounts for a large proportion of the observed hydraulic variability with errors comparable to other 2-D model studies. Given the uncertainty associated with survey procedures (±0.02 m) and field velocity measurements, the errors of 0.05, 0.08, and 0.03 m depth and 0.04, 0.04, and 0.05 m/s velocity at the three low flow TBAR cross sections depth and velocity at the TBAR are considered adequate **(Fig. 8)**.

7.3. Habitat Modeling

Model predictions of habitat suitability at the TBAR were substantiated by redd surveys. Redds are consistently located near predicted good and excellent habitat zones throughout the site and areas predicted to have poor habitat suitability lack any significant number of redds **(Fig. 10)**. Where the model predicts small areas (<1m²) of habitat along the complex side channel, salmon redds were observed. This suggests salmon can locate and utilize extremely localized hydraulic conditions and that the HSC methodology is capable of resolving such features. Therefore, the model was able to capture both wide scale patterns of habitat suitability associated with meso-scale features (e.g. riffle entrances) and smaller micro-scale conditions along the complex side channel. Results from the electivity calculations further support the use of Mokelumne River HSCs **(Fig. 11)**. The low electivity values for poor and fair habitat suggest an overabundance of poor and fair habitat at the TBAR with only minor utilization. The values of 1.61 and 3.56 for the good and excellent habitat classes suggest utilization proportionally exceeds availability and that a preference for these GHSI values was observed. Overall, the Mokelumne River HSC model accurately predicted both the pattern of habitat suitability and the observed preference and avoidance behaviors of spawning Chinook salmon at the TBAR.

7.4. Bed Material

7.4.1. Hypothesis H_1

Although not accounted for in the habitat suitability indices in this study, sediment size distributions are key selection variables for spawning salmonids. The suitability of gravels is a function of species, fish size, and specific hydraulic conditions including

upwelling near the bed where female salmon interact with the substrate (Giest and Dauble, 1998; Kondolf, 1993). For instance, higher near-bed velocities enable anadromous fish to excavate larger particles by using the increased momentum of the flow. The basic analysis and comparison provided does not account for this dynamic relationship between velocity, upwelling, and other parameters on the suitability of gravel at each site. Instead the analysis assumes a suitable gravel size defined by past studies.

At the EDR, Englebright Dam has blocked off all coarse sediment input. This caused what Kondolf (1997) termed "hungry water", where suitable spawning gravels are winnowed away leaving only coarse, resistant particles. The remaining bed consists of stable blast rock and resembles rip rap used to bolster eroding levees and seashores. Only 25% of bed particles are within the reported suitable range of 12-80 mm for spawning Chinook salmon at the EDR compared to nearly 50% at the TBAR. Although one quarter of sediments at the EDR might be available to salmon, this value masks the fact that all recorded gravels were highly angular and thus less suitable for spawning salmonids. All comparisons of sediment classes using the Wilcoxon-Mann-Whitney test had alpha values below 0.05 except for the D_{16} analysis. The reported alpha value was slightly higher than the threshold for rejection (0.057 versus 0.05). Overall, H_1 is rejected due to statistical differences between the study sites and the reduced quantity and quality of spawning gravels within the known preference range of Chinook salmon at the EDR.

The rejection of H_1 suggests that if mitigation goals are to increase habitat in the 1.5 km reach between Englebright and Deer Creek, the issue of sediment deficiency must be resolved. GA will alter the sediment size distribution at the site through direct injection of size sorted gravels from quarries nearby. In this respect GA is a direct manipulation of

a channel input that will skew the sediment component of habitat. However, as mentioned above, the simple injection of gravels does not guarantee that habitat conditions will improve; ultimately the in-stream geomorphic processes of entrainment and deposition determine where gravels deposit and whether they form usable spawning habitat.

7.5. Hydraulics

7.5.1. Hypothesis H_2

H_2 is rejected because a velocity reversal associated with an upstream constriction is not observed at the EDR **(Fig. 14)**. Flow convergence routing is focusing high Shields stress over the constricted run across all discharges and keeping Shields stresses over the pools lower. Consequently, injected gravel would never deposit on the high bedrock shelves directly below the two pools in the DEM. These results show that for all modeled flows valley constriction is the dominant geomorphic factor controlling hydraulics and sediment transport in the EDR, and that was also found to be the controlling factor at the TBAR. The lateral constriction at the EDR causes the location of maximum velocity to change little with increasing discharge and produces significant differences in sediment transport between the EDR and TBAR. For example, valley constriction causes Shields stress values in the full transport range (0.06-0.1) to occur at a discharge of 710.7 m^3/s at the EDR but not until somewhere between 998 m^3/s and 3089 m^3/s for the TBAR **(Fig. 17 & Fig. 19)**. From the perspective of GA, the effect of valley constriction on hydraulics and transport at the EDR will cause gravels mobilized upstream of the run to be transported over the topographic controls identified in the DEM

and through the run with only minor deposition in micro-scale depositional environments (e.g., boulder shadows).

7.6. Geomorphology

7.6.1. Hypothesis H_3-H_6

In general, Shields stress values above 0.06 ($\tau^* > 0.06$) represent full transport of the channel bed and are expected to produce considerable morphologic change. A significant portion of the channel is not in the full transport regime for the 22.6, 33.7 or 271.3 m³/s events: H_3 and H_4 are accepted. For the spawning flows, scour and evacuation of particles does not occur and habitat features formed via GA and high-flows will be stable. A biologically important consequence is that redd scour and reduced survival of embryos during frequent low intensity events should not be a management concern. However, morphologic change resulting from GA will alter the location and percent of channel experiencing full transport. Therefore, velocity and Shields stress values after gravel augmentation should be recognized as important factors to consider when limiting the loss of eggs and developing embryos.

Although significant full transport was not predicted for the EDR 271.3 m³/s event, partial transport covered ~10% of the wetted channel. At this discharge mid-channel habitat will start to degrade under current conditions. Intermittent and partial transport in the run could potentially scour redds in the channel center and poses a major restriction on GA efficacy to be discussed later. To determine the potential risk for redd scour, an investigation that blends the conceptual understanding of Montgomery (1996) and

FESWMS's sediment transport module could provide typical scour depths for any flow and better quantify the effects on salmonids if GA led to mid-channel habitat formation.

Stability of the channel bed during low flows does not infer rehabilitation success and instead brings up the issue of temporal efficacy. If GA proceeds and is followed by extensive low flow periods, habitat features will not form. For instance, current logistical constraints limit gravel additions to the tail of the Narrows II afterbay where intermittent transport is not predicted until discharge exceeds 271.3 m^3/s. This suggests a characteristic lag between the time of investment (injection of gravels) and entrainment that can be approximated by investigating Shields stress in the Narrows pool at lower frequency (higher discharge) events.

During the 900.5 m^3/s (5-year) event, more than 10% of the channel was in the full transport regime. At this discharge, velocities in the Narrows II afterbay are large enough to entrain and transport particles downstream. Therefore, a rough estimate for the lag between injection and significant entrainment is 5 years. Overall, H_5 is rejected at the EDR with the primary location of full transport corresponding to the run section of the channel. Similar to the 271.3 m^3/s discharge, a 5-year event will tend to degrade channel morphology and scour redds in the run. Although H_5 is rejected, full transport is highly localized, and the no, intermittent, and partial transport regimes predicted along channel edges suggests margin areas are less susceptible to scour.

With over 52% of the channel in the full transport class at a discharge of 2588.2 m^3/s (24-year event), H_6 is rejected. The consequences to habitat are more extreme than the 5-year event and overall augmented gravels can be expected to move as a carpet along the resistant bed. An event equal or exceeding this magnitude would pose a serious concern

for incubating eggs or larval fish residing within gravel interstices. The rejection of H_5 and H_6 suggest spawning habitat formed in the channel center should not be a rehabilitation priority.

7.6.2. Hypothesis H_7

Historical photos near EDR before the construction of Englebright Dam elicit valuable information about the underlying geomorphic character of the site and provide a starting point for evaluating system response to GA. For instance, although a large amount of sediment, ~522 million m³ from the South Yuba alone, was forced into the Yuba as a consequence of hydraulic mining, the site lacks large deposits or bars of exposed gravel and cobbles in the 1909 photo **(Fig. 20)**. This suggests transport capacity at the EDR was not lacking before the construction of Englebright and that the reach was supply limited even with the flux of hydraulic mine debris. The hydrologic event analysis furnished above **(Fig. 4)** and the corresponding Shields stress predictions for the modeled discharges suggest the EDR will continue to operate as a supply limited reach.

The sediment deposition patterns depicted in **Fig. 20** have profound consequences on GA efficacy in at the EDR and other bedrock channels. Instead of widespread aggradation in riffle and run sequences, gravel deposition will preferentially occur in conjunction with resistant bed-forms and boulder particles. For example, at the EDR the underlying topography and roughness elements create localized areas of upwelling and lateral vortices that facilitate deposition much like the site shown in Gilbert's 1909 image. This finding agrees with the concept of "nested depositional features" proposed by McBain (2004) and "gravel beaches" by Wohl (1998). Originally, McBain (2004)

suggested these features were deterministically organized by the dominant flow regime, however in reality stochasticity likely plays a larger role. Overall, the available historical images indicate that heterogeneous patterns of deposition and habitat, correlated to underlying topographical control, will occur after GA.

Comparing historical and current images can further clarify the possible response of the channel to GA. **Figure 22A** and **22B** represent ~100 years of change in the reach directly below EDR. Prior to the completion of Englebright, coarse substrate was ubiquitous between what is now the Narrows I powerhouse and Deer Creek. A large pool and riffle sequence with underlying gravel substrate dominateed the Deer Creek confluence. Despite an increase in valley width downstream of the EDR, which may have contributed to aggradation, the comparison suggests an underlying behavior of the channel. As upper watershed sediment inputs were cut off, the remaining stream power of the Yuba River gradually evacuated hydraulic mine sediments from the site. The entrainment and deposition of blast rock depicted in **Fig. 21** over the time period signifies an innate high transport capacity that will certainly distribute augmented gravels downstream.

The post Englebright estimated sediment transport numbers for the EDR and TBAR provide another insight regarding system response to GA. The estimations should not serve as goals for mitigation efforts that if reached will elicit permanent habitat improvements at the site. The EDR gravel budget of 47124 m^3/yr and volumetric differencing at the TBAR of 19984 m^3 for the 24-year event reflect inputs of hydraulic mine debris that increased delivery of sediments to channels throughout the Sierra Nevada. Consequently each number is likely an overestimation of natural sediment

delivery. Instead the numbers should serve as reference for overall channel transport capacity to conjure and analyze mitigation objectives. For example GA on the scale of 47124 m^3/yr would cost roughly 1.2 million dollars annually in washed gravel assuming the same material and delivery price of $14/ton as projects on the Mokelumne River, Ca. This high cost, (especially since it does not include transportation and injection) suggests that matching augmentation to pre-dam volumetric delivery would be a costly objective to pursue given the risk of gravels vacating the site in a single year.

The cost of matching channel inputs to sediment transport estimations underscores the importance and necessity of pilot gravel injections and adaptive management. Small GA projects like the one completed in the fall of 2007 at the EDR can test modeling predictions of transport and deposition against habitat development through pre and post project assessments. For instance, although Shields stress predictions suggest that mid-channel habitat will preferentially deteriorate at the EDR, subsequent deposition on riffle sequences downstream of the study site might create habitat over longer temporal scales that only continuous monitoring can capture. If this is the case, the investment of 1.2 million dollars per year may be a viable option to pursue.

A final comparison of Shields stress values in the EDR spawning channel against transport processes at the TBAR provides further evidence that extensive cross channel habitat will not develop at the EDR. Shields stress patterns in **Fig. 24** show the channel mid-section is the most active part of the site and that for all flows, once entrainment begins in the pool, particles will funnel through pool tail and run sections. Without an upstream sediment source and dynamic Shields stress distribution, riffle habitat that forms at the tail of the Narrows II pool and in the channel center will not be stable and

will rapidly degrade. This is in sharp contrast to the TBAR, where a significant source of sediment for maintenance of topographical relief exists and dynamic transport process scours pools and deposits sediments near the riffle crest during high flows. This fundamental difference suggests that habitat formation at the EDR is not dominated by flow convergence routing and an associated velocity reversal. Therefore, the transport dominated character of the bedrock EDR will prohibit large scale aggradation in the spawning channel and H_7 is rejected.

From a management perspective two broad conclusions regarding GA efficacy can be drawn from these results. First, mitigation measures aimed at increasing spawning habitat at the EDR should focus on channel margin areas and the depositional features where natural processes promote gravel deposition. The second conclusion is that habitat formed via GA will be spatially limited due to the patchy and heterogeneous character of depositional features in bedrock canyon channels.

7.7. Habitat

7.7.1. Hypothesis H_8

Historical data of spawning on the Yuba river includes the general locations and physical barriers to migrating salmonids (Yoshiyama et al., 1998). Although extremely valuable, the literature provides little information about specific spawning activity at the project site investigated in this study. In general, salmonids prefer to spawn in homogeneous lower gradient gravel-bed channels, however, micro scale heterogeneity (10^0-10^1 channel widths) is important and provides a range of hydraulic conditions for spawning, resting, and juvenile rearing. Kondolf (1991) investigated the spawning

habitat of brown trout (*Salmo trutta*) and rainbow trout (*Onchorhynchus mykiss*) in boulder-bed channels of the eastern Sierra Nevada. Although the research was not on Chinook salmon habitat, the conclusions drawn from that study are similar to those encountered at the EDR. Kondolf (1991) found that highly localized patches of habitat formed near natural hydraulic controls or roughness elements in the channel that promoted sediment deposition. Given the distribution of sediment particles in historical images and Shields stress predictions, spawning at the EDR was likely limited to similar highly localized areas. Therefore, both the geomorphic and ecologic evidence suggests widescale spawning at the EDR did not occur; H_8 is rejected.

The observations of successful Chinook spawning near the EDR in the 1970s and 1980s and of brown and rainbow trout by Kondolf (1991) both represent the ability of salmonid species to locate and utilize patchy habitat features in bedrock systems. In the Yuba River example, hydraulic mining provided ample sediments to fill localized depositional zones and likely increased habitat suitability. Successive flood events have since degraded the depositional features and explain the complete lack of observed redds in over fifteen visits to the EDR spanning the 2005 and 2007 spawning seasons. GA will reconnect the sediment component of channel inputs, and restore some of the patchy depositional features in the channel.

7.7.2. Hypothesis H_9

Model predicted habitat at the two project sites differed quantitatively and qualitatively. The large proportion of good and excellent quality areas at the TBAR (~34% of area) and a lack of redd superposition issues suggests that spawning habitat is

not limiting there. However, at the EDR less than 3% of the channel was within the same good and excellent quality suitability classes (based on hydraulics alone) and therefore H_9 is rejected; spawning habitat at the EDR is severely limited. Given the vast differences of channel response to increasing discharge, bed mobility (Shields stress), sediment input, and large scale topographic control between the EDR and TBAR, one cannot assume that the proportion of suitable habitat should be similar at the two sites (Buffington et al., 2004). The quantitative comparison is most useful in that it shows the differing capacity of each site to harbor spawning and serves as a baseline value of habitat at the EDR prior to any rehabilitation efforts.

By breaking spawning habitat into two general groups at each site, one associated with riffle entrances and the other with margin habitat, a distinct difference in the proportion of habitat types is apparent. Good and excellent habitat at the TBAR is dominated by riffle entrances while at the EDR all good and excellent quality habitat can be attributed to margin zones parallel to the channel edge where the combination of edge topography and water depth create suitable hydraulic conditions. Depths within the channel center and pool exits are too great given the low velocity values predicted with the model. Therefore, suitable spawning habitat was only predicted within two meters of the channel margin. Shields stress predictions suggest that alluvial deposition is most likely to occur along and adjacent to these channel margins where depth is currently limiting spawning habitat. Any alluvial deposition that occurs along channel margins may increase overall spawning habitat via a decrease in depth and increase in velocity at the EDR. Interestingly, similarly sized (<1m) strips of margin habitat exists at the TBAR where riffle entrance habitat is not limiting and redd surveys have confirmed the ability

of Chinook salmon to utilize these narrow strips. This suggests that if the issue of sediment size and depth limitations within margin zones at the EDR could be resolved, spawning activity would be promoted on a localized scale.

8. CONCLUSION

The precipitous decline of anadromous fish species throughout the Pacific Northwest is widely attributable to hydrologic, geomorphic, and ecologic discontinuities. GA has been a successful rehabilitation technique in many regulated gravel bed rivers and its extension to bedrock canyon channels has been investigated herein. The efficacy of GA is a complex function of channel hydraulics, sediment supply/transport, local topographic control, and high flow events in regulated systems.

For the bedrock canyon channel at the EDR, the underlying transport dominated character, as evidenced through Shields stress predictions and the remaining dynamic flow regime, will have two overarching impacts on augmentation efficacy. First, it guarantees augmented gravels will be distributed downstream with intermittent transport of particles predicted near the 5-year event discharge. Second, and most importantly, valley wall constrictions and depositional features dominate deposition processes and force velocity and Shields stress values to their maximums near the channel thalweg for all modeled scenarios. This will suppress the formation of cross channel gravel riffles that begin to scour during relatively frequent (Q_2 and Q_5) events. Instead of creating riffle spawning habitat, GA in the bedrock canyon channel at the EDR will likely produce patchy heterogeneous habitat along channel margins and recirculation zones where depositional features impact local hydraulics.

Overall, small scale GA at the bedrock dominated EDR is not expected to significantly increase the proportion of channel available for spawning salmon despite the small (1 m^2) localized zones of habitat that are likely to form. Unlike gravel-bed rivers directly below impoundments, where the creation of macro-scale bed features such as riffles and spawning beds have been highly successful, such features are not promoted in the active bedrock channel investigated here. However, small scale habitat features that result from gravel augmentation may be disproportionately important to the endangered spring-run Chinook salmon that have had historic spawning areas cut off by impoundments. To determine if augmented gravels increase spawning habitat at the EDR or form macro-scale habitat features (e.g., riffles) outside of the EDR domain, the continued monitoring of injected gravels and salmon utilization along the 1.5 km reach below Englebright Dam is recommended.

9. REFERENCES

Banks, M.A., Rashbrook, V.K., Valavetta, M.J., Dean, C.A. and Hedgecock, D., 2000. Analysis of microsatellite DNA resolves genetic structure and diversity of chinook salmon *(Oncorhynchus tshawytscha)* in California's Central Valley. Canadian Journal Fisheries and Aquatic Sciences, 57: 915-927.

Baxter, R.M., 1977. Environmental Effects of Dams and Impoundments. Annual Review of Ecology and Systematics, 8: 255-283.

Bernhardt, E.S. et al., 2005. Synthesizing U.S. River Restoration Efforts. Science, 308.

Brandt, S.A., 2000. Classification of Geomorphological Effects Downstream of Dams. Catena, 40: 375-401.

Brown, A.V., Lyttle, M.M. and Brown, K.B., 1998. Impacts of Gravel Mining on Gravel Bed Streams. Transactions of the American Fisheries Society, 127: 979-994.

Brown, R.A. and Pasternack, G.B., 2008. Engineered Channel Controls Limiting Spawning Habitat Rehabilitation Success on Regulated Gravel-bed Rivers. Gemorphology, 97: 631-654.

Buffington, J.M., Montgomery, D.R. and Greenberg, H.M., 2004. Basin-scale Availability of Salmonid Spawning Gravel as Influenced by Channel Type and Hydraulic Roughness in Mountain Channels. Canadian Journal Fisheries and Aquatic Sciences, 61: 2085-2096.

Bunn, S.E. and Arthington, A.H., 2002. Basic Principles and Ecological Consequences of Altered Flow Regimes for Aquatic Biodiversity. Environmental Management, 30(4): 492-507.

Bunte, K., 2004. State of the Science Review, Gravel Migration and Augmentation Below Hydroelectric Dams : A Geomorphological Perspective, USDA Forest Service, Fort Collins, CO.

Cada, G.F. and Sale, M.J., 1993. Status of Fish Passage Facilities at Nonfederal Hydropower Projects. Fisheries, 18(7): 4-12.

CDFG, 1991. Lower Mokelumne River Fisheries Mangement Plan, California Department of Fish and Game. Resource Agency, Sacramento, California.

CDWR, 1992. Project Report: Sacramento River Spawning Gravel Restoration Phase 1, California Department of Water Resources. Northern District.

CDWR, 2006. Upper Yuba River Watershed Chinook Salmon and Steelhead Habitat Assessment Technical Report. Upper Yuba River Studies Program Study Team.

Chow, V.T., 1959. Open-channel hydraulics. McGraw-Hill, New York, 680 pp.

Collier, M., Webb, R.H. and Schmidt, J.C., 1996. Dams and River: Primer on the Downstream Effects of Dams. Circular 1126, U.S. Geological Survey, Menlo Park, CA.

Crisp, D.T., 1987. Thermal ' Resetting ' of Streams by Reservoir Releases with Special Reference to Effects on Salmonid Fishes. Regulated Streams: Advances in Ecology. Plenum Press, New York, p 163-182 pp.

Ebbersole, J.L., Liss, W.J. and Frissell, C.A., 1997. Restoration of Stream Habitats in the Western United States: Restoration as Reexpression of Habitat Capacity. Environmental Management, 21(1): 1-14.

Elkins, E.M., Pasternack, G.B. and Merz, J.E., 2007. Use of Slope Creation for Rehabilitating Incised, Regulated, Gravel Bed Rivers. Water Resources Research, 43(W05432): 16.

Emmett, W.W. and Wolman, G.M., 2001. Effective Discharge and Gravel-Bed Rivers. Earth Surface Processes and Landforms, 26: 1369-1380.

Freeman, G.E., Rahmeyer, W.H. and Copeland, R.R., 2000. Determination of Resistance Due to Shrubs and Woody Vegetation, U.S. Army Core of Engineers Technical Report. ERCD/CHL TR-00-25.

Friedman, J.M., Osterkamp, W.R., Scot, M.L. and Auble, G.T., 1998. Downstream Effects of Dams on Channel Geometry and Bottomland Vegetation:Regional Patterns in the Great Plains. Wetlands, 18(4): 619-633.

Froehlich, D.C., 2002. Finite Element Surface-Water Modeling Systems: Two-dimensional Flow in a Horizontal Plane--Users Manual. Federal Highway Administration Report FHWA-RD-88-177, pp. 285.

Ghanem, A., Steffler, P., Hicks, F. and Katopodis, C., 1996. Two-Dimensional hydraulic simulation of physical habitat conditions in flowing streams. Regulated Rivers:Research and Management, 12: 185-200.

Giest, D.R. and Dauble, D.D., 1998. Redd Site Selection and Spawning Habitat use by fall Chinook salmon: the importance of Geomorphic features in large rivers. Environmental Management, 22(5): 655-669.

Graf, W.L., 1999. Dam Nation: A geographic census of American dams and their large-scale hydrologic impacts. Water Resources Research, 35(4): 1305-1311.

Grant, G., Burkholder, B., Jefferson, A., Lewis, S. and Haggerty, R., 2006. Hyporheic Flow, temperature anomalies, and gravel augmentation: Preliminary findings of a field investigation on the Clackamas River, Oregon, Pacific Northwest Research Station (USFS) and Oregon State University.

Groot, C. and Margolis, L., 1991. Pacific salmon life histories. University of British Columbia Press, Vancouver, Canada.

Harper, D., Ebrahimnezhad, M. and Cot, F.C.I., 1998. Artificial riffles in river rehabilitation: setting the goals and measuring the successes. Aquatic Conservation-Marine and Freshwater Ecosystems, 8(1): 5-16.

Heil, R.J. and Brych, S.M., 1978. An approach for consistent topographic representation of varying terrain, American Society of Photgrammetry: Digital Terrain Models Symposium, St. Louis, Missouri, pp. 397-411.

Horritt, M.S., Bates, P.D. and Mattinson, M.J., 2006. Effects of mesh resolution and topographic representation in 2D finite volume models of shallow water fluvial flow. Journal of Hydrology, 329(1-2): 306-314.

Ipson, M.K., 2006. Analysis of the Sediment Transport Capabilities of FESWMS FST2DH. Maters Thesis, Brigham Young University, Provo.

Ivlev, V.W. (Editor), 1961. Experimental Ecology of the feeding of fishes. Yale University Press, New Haven, 302 pp.

James, A., 2002. Late Pleistocene Glaciations in the Northwestern Sierra Nevada, California. Quaternary Research, 57(3): 409-419.

James, A., 2005. Sediment from hydraulic mining detained by Englebright and small dams in the Yuba basin. Geomorphology, 71(1-2): 202-226.

James, A., 2007. Yuba River Aerial Imagery 1937-1952. Personal Communication.

Keller, E.A., 1971. Areal Sorting of bed-load material: the hypothesis of velocity reversal. Geological Society of America Bulletin, 82: 723-756.

Kondolf, G.M., and Li, S., 1992. The Pebble Count Technique for Quantifying Surface Bed Material Size in Instream Flow Studies. Rivers, 3(80-87).

Kondolf, G.M., and M.G. Wolman, 1993. The sizes of salmonid spawning gravels. Water Resources Research, 29: 2275-2285.

Kondolf, G.M., and M.G. Wolman, 1998. Lessons learned from river restoration projects in California. Aquatic Conservation: Marine and Freshwater Ecosystems, 8: 39-52.

Kondolf, G.M., Cada, G.F., Sale, M.J. and T., F., 1991. Distribution and Stability of Potential Salmonid Spawning Gravels in Steep Boulder-Bed Streams of the Eastern Sierra Nevada. Transactions of the American Fisheries Society, 120(2): 177-186.

Kondolf, G.M., Larson, M., 1995. Historical channel analysis and its application to riparian and aquatic habitat restoration. Aquatic Conservation: Marine and Freshwater Ecosystems, 5(2): 109-126.

Kondolf, G.M., M.W. Smeltzer, Railsback, 2001. Design and Performance of a Channel Reconstruction Project in a Coastal California Gravel-Bed Stream. Environmental Management, 28(6): 761-766.

Kondolf, M.G., 1997. Hungry Water: Effects of dams and gravel mining on river channels. Environmental Management, 21(4): 533-551.

Kondolf, M.G., 2004. Coarse sediment augmentation on the Trinity river below Lewiston dam: Geomorphic perspectives and review of past projects.

Kulpa, J., 2006. Environmental Data Solutions. Personal Communication.

Lee, J., 1991. Comparison of existing methods for building triangular irregular network models of terrain from grid digital elevation models. International Journal of Geographic Information Systems, 5(3): 267-285.

Ligon, F.K., Dietrich, W.E. and Trush, W.J., 1995. Downstream Ecological Effects of Dams. Bioscience, 45(3): 183-192.

Lisle, T.E., Nelson, J.M., Pitlick, J., Madej, M.A. and Barkett, B.L., 2000. Variability of bed mobility in natural, gravel-bed channels and adjustments to sediment load at local and reach scales. Water Resources Research, 36(12): 3743-3755.

MacWilliams, M.L., Wheaton, J.M., Pasternack, G.B., Street, R.L. and Kitanidis, P.K., 2006. Flow convergence routing hypothesis for pool-riffle maintenance in alluvial rivers. Water Resources Research, 42(W10427).

McBain, S. and Trush, B., 2004. Attributes of Bedrock Sierra Nevada River Ecosystems. U.S. Department of Forest Service.

Merz, J.E., Chan, Leigh H. Ochikubo, 2005. Effects of gravel augmentation on macroinvertebrate assemblages in a regulated California river. River Research and Applications, 21(1): 61-74.

Merz, J.E., Pasternack, G. B., Wheaton, J. M., 2006. Sediment Budget for Salmonid Spawning Habitat Rehabilitation in the Mokelumne River. Geomorphology, 76(1-2): 207-228.

Merz, J.E., Setka, J.D., Pasternack, G.B. and Wheaton, J.M., 2004. Predicting benefits of spawning-habitat rehabilitation to salmonid (Oncorhynchus spp.) fry production

in a regulated California river. Canadian Journal of Fisheries and Aquatic Sciences, 61(8): 1433-1446.
Mesick, C., 2002. Knights Ferry Gravel Replenishment Project. Project # 97-N21, Cal Fed Bay Delta Program.
Miller, A.J. and Cluer, B.L., 1998. Modeling considerations for simulation of flow in bedrock channels. In: Rivers over rock: fluvial processes in bedrock channels. American Geophysical Union Monograph #107, Washington, DC.
Minear, T.J. and Kondolf, G.M., 2006. Gravel Augmentation for Salmon Habitat Below Dams in Northern California. Presentation.
Moir, H.J. and Pasternack, G.B., 2008. Relationships between mesoscale morphological units, stream hydraulics and Chinook salmon (Oncorhynchus tshawytscha) spawning habitat on the Lower Yuba River, California. Geomorphology.
Montgomery, D.R., 2000. Coevolution of the Pacific Salmon and Pacific Rim Topography. Geological Society of America Bulletin, 28(12): 1107-1110.
Montgomery, D.R., Buffington, J.M., Peterson, P.N., Schuett-Hames, D. and Quinn, T.P., 1996. Stream-bed scour, egg burial depths, and the influence of salmonid spawning on bed surface mobility and embryo survival. Canadian Journal Fisheries and Aquatic Sciences, 53: 1061-1070.
Mullican, R., 2007. Personal Communication, Private Landowner and Yuba County Resident.
Paintal, A.S., 1971. Concept of critical shear stress in loose boundary open channels. Journal of Hydraulic Research, 9(1): 91-113.
Pasternack, G.B., Gilbert, A., Wheaton, J.M. and Buckland, E., 2006. Error Propagation for velocity and shear stress prediction using 2 D models for environmental management. Journal of Hydrology, 328(1-2): 227-241.
Poff, L.N. et al., 1997. The Natural Flow Regime: A paradigm for river conservation and restoration. Bioscience, 47(11): 769-784.
Power, M.E., Dietrich, W.E. and Finlay, J.C., 1996. Dams and downstream aquatic biodiversity: potential food web consequences of hydrologic and geomorphic change. Environmental Management, 20: 887-895.
Rameshwaran, P. and Shiono, K., 2003. Computer modelling of two-stage meandering channel flows, Proceedings of the Institution of Civil Engineers - Water and Maritime Engineering, pp. 325-339.
Rathburn, S. and Wohl, E., 2003. Predicting fine sediment dynamics along a pool-riffle mountain channel. Geomorphology, 55: 111-124.
Richter, B.D., and G. A. Thomas, 2007. Restoring environmental flows by modifying dam operations. Ecology and Society, 12(1): 12.
Richter, B.D., Baumgartner, J.V., Powell, J. and Braun, D.P., 1996. A Method for Assessing Hydrologic Alteration within Ecosystems. Conservation Biology, 10(4): 1163-1174.
Richter, B.D., Baumgartner, Jeffrey V., Powell, Jennifer, and Braun, David, P., 1997. How much water does a river need? Freshwater Biology, 37: 231-249.
Rosgen, D.L., 1985. A Stream Classification System, First North American Riparian Conference, Tucson, AZ, pp. 91-95.

Scruton, D.A., 1996. Evaluation of the construction of artificial fluvial salmonid habitat in a habitat compensation project, Newfoundland, Canada. Regulated Rivers-Research & Management, 12(2-3): 171-183.

Slater, D.W., 1963. Winter-run Chinook salmon in the Sacramento River, California with notes on water temperature requirements at spawning., U.S. Fish and Wildlife Service, Washington, D.C.

Snyder, N.P. and Rubin, D.M., 2004. Estimating accumulation rates and physical properties of sediment behind a dam: Englebright Lake, Yuba River, northern California. Water Resources Research, 40.

Stanford, J.A. et al., 1996. A general protocol for restoration of regulated rivers. Regulated Rivers:Research and Management, 12: 391-413.

Talbert, T., 1999. Yuba Goldfields Fish Barrier Project:Preliminary Engineering Report, California Department of Water Resources, Yuba County, CA.

USGS, 2006. U.S. Geological Survey Photographic Library, http://libraryphoto.cr.usgs.gov/photo_all.htm.

Wang, C.L., Pasternack, G.B. and Merz, J.E., 2004. Application of a 2-D Hydraulic Model to Reach-scale Spawning Gravel Rehabilitation. River Research and Applications, 20(2): 205-225.

Ward, J.V. and Stanford, J.A., 1995. Ecological connectivity in alluvial rivers and its disruption by flow regulation. Regulated Rivers:Research and Management, 11: 105-119.

Wheaton, J.M., Pasternack, G.B. and Merz, J.E., 2004a. Spawning Habitat Rehabilitation-II. Using Hypothesis Testing and Development in Design, Mokelumne River , CA USA. International Journal of River Basin Management, 2: 21-37.

Wheaton, J.M., Pasternack, G.B., Merz, J.E., Garcia de Jalon Lastra, D. and Martinez, P.V., 2004b. Use of habitat heterogeneity in salmonid spawning habitat rehabilitation design, Fifth International Symposium on Ecohydraulics, Aquatic Habitats: Analysis & Restoration, Madrid, pp. 791-796.

Wheaton, J.M., Pasternack, G.B., Merz, Joseph, 2004. Spawning habitat rehabilitation-1 Conceptual approach and methods. International Journal River Basin Management, 2(1): 3-20.

Whipple, K.X., 2001. Fluvial landscape response time: How plausible is steady-state denudation? American Journal of Science, 301(4-5): 313-325.

Williams, G.P. and Wolman, G.M., 1984. Downstream effects of dams on alluvial rivers. U.S. Department of the Interior, Geological Society, Professional Paper #1286.

Wohl, E. et al., 2005. River Restoration. Water Resources Research, 41.

Wohl, E. and Tinkler, K.J., 1998. A Primer on Bedrock Channels. In: Rivers over rock: fluvial processes in bedrock channels. Geophysical Monograph Series #107

Wolman, M.G., 1954. A Method of Sampling Coarse River-bed Material. Transactions of the American Geophysical Union, 35: 951-956.

Yoshiyama, R.M., Moyle, P.B. and Fisher, F.W., 1998. Historical Abundance and Decline of Chinook Salmon in the Central Valley Region of California. North American Journal of Fisheries Management, 18(3): 487-521.

Zeh, M. and Donni, W., 1994. Restoration of Spawning Grounds for Trout and Grayling in the River High-Rhine. Aquatic Sciences, 56(1): 59-69.

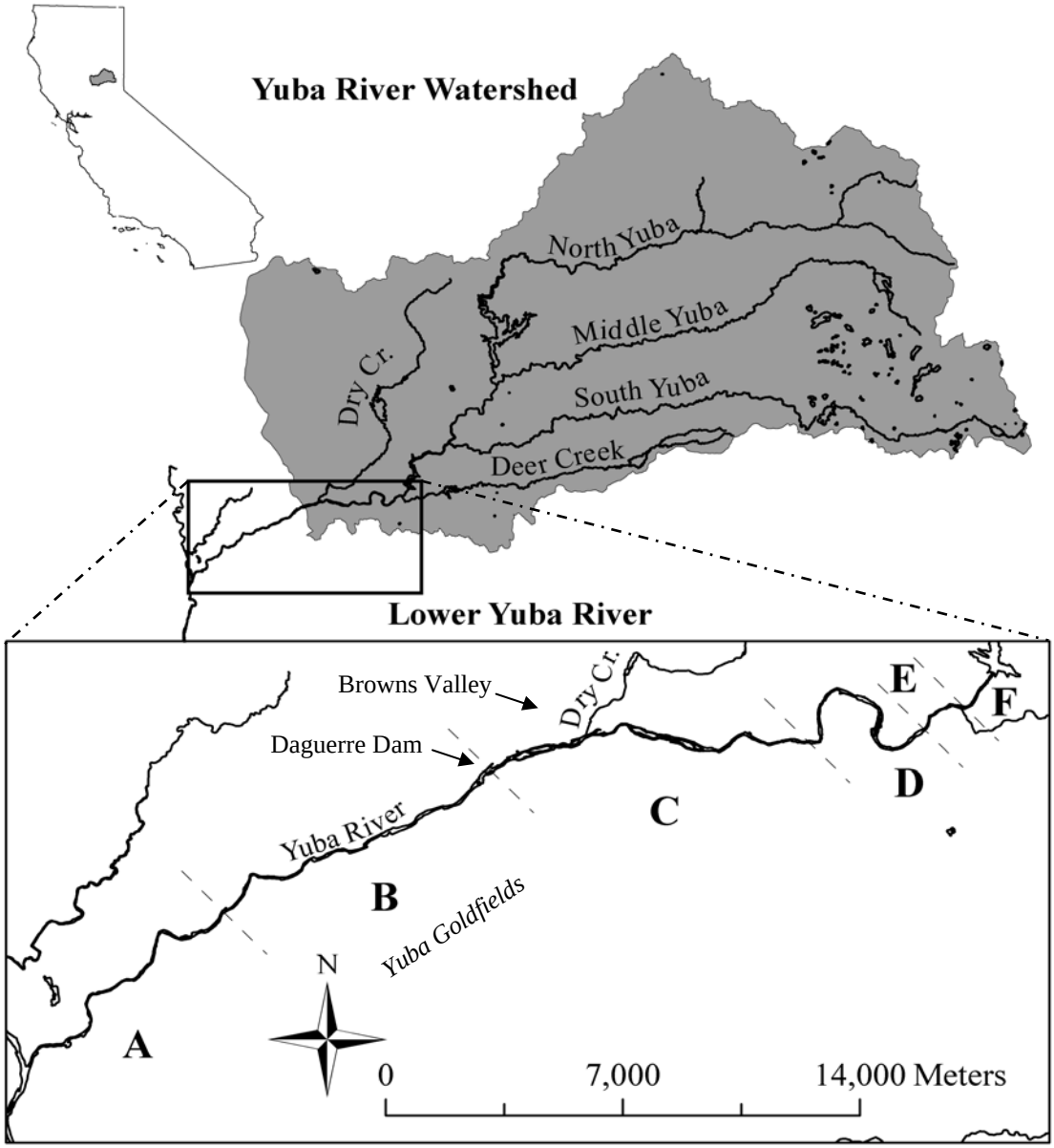

Figure 1. The Yuba River watershed and its tributaries are located on the western slope of California's northern Sierra Nevada Mountain Range (top). The six sections of the Lower Yuba River include A) the Simpson Lane, B) Daguerre Dam, C) Highway 20, D) Timbuctoo Bend, E) Narrows, and F) Englebright Dam reaches (bottom).

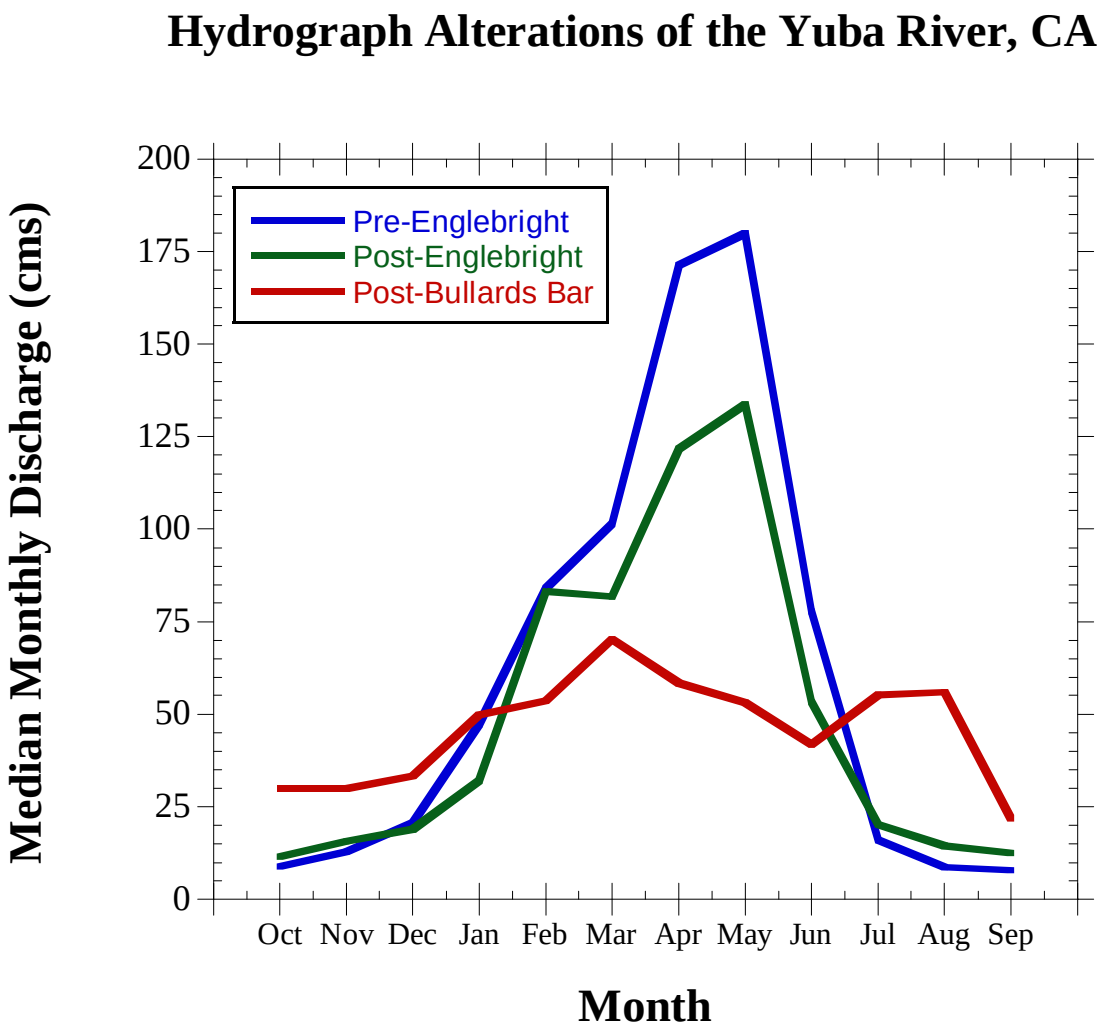

Figure 2. Median monthly discharge for the Smartville gages (#11418000 and #11419000) during the three major hydrologic periods spanning 1904-2006.

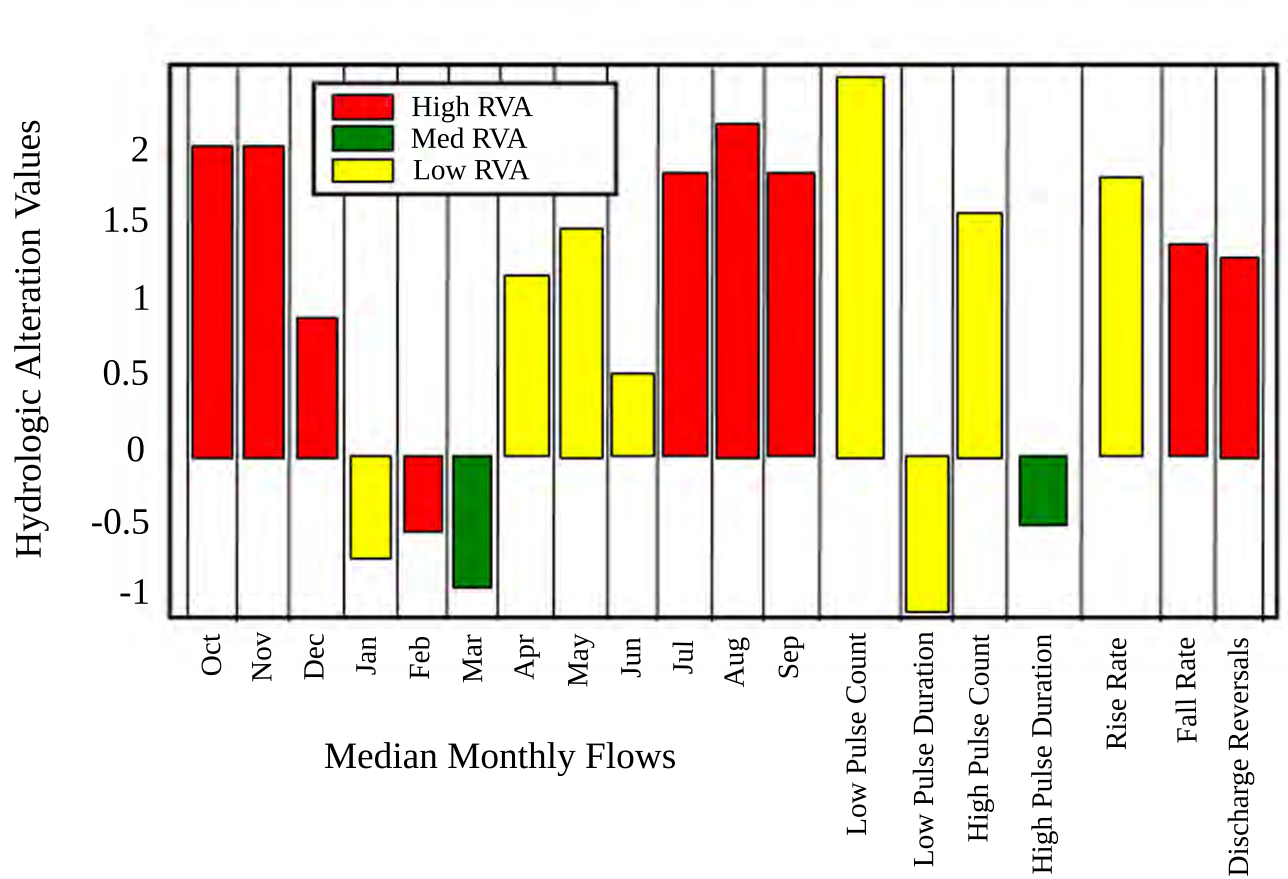

Figure 3. Output from the non-parametric form of Indicators of Hydrologic Alteration (Richter, 1996) using Yuba river discharge data before and after the construction of New Bullards Bar Dam.

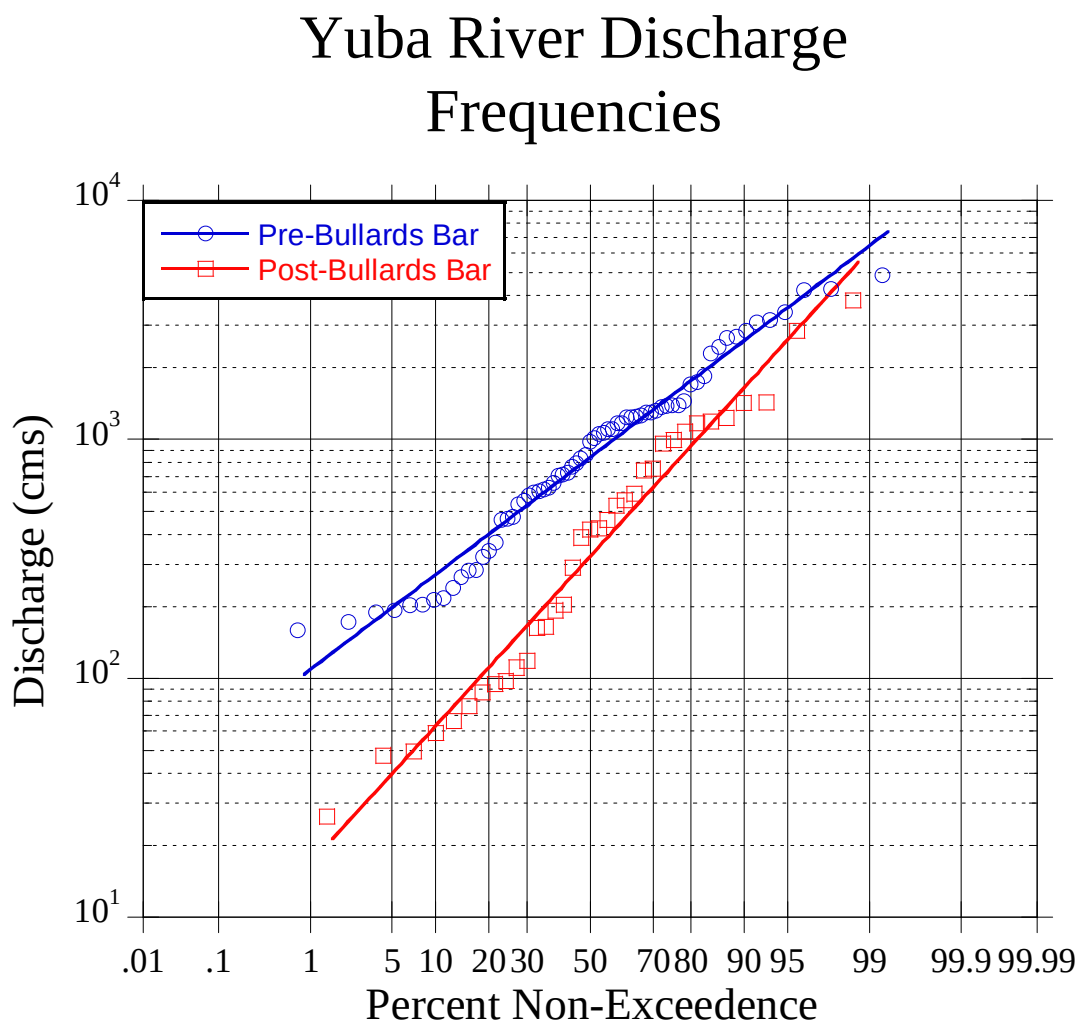

Figure 4. Reduction in annual peak discharge frequencies following the construction of New Bullards Bar Dam.

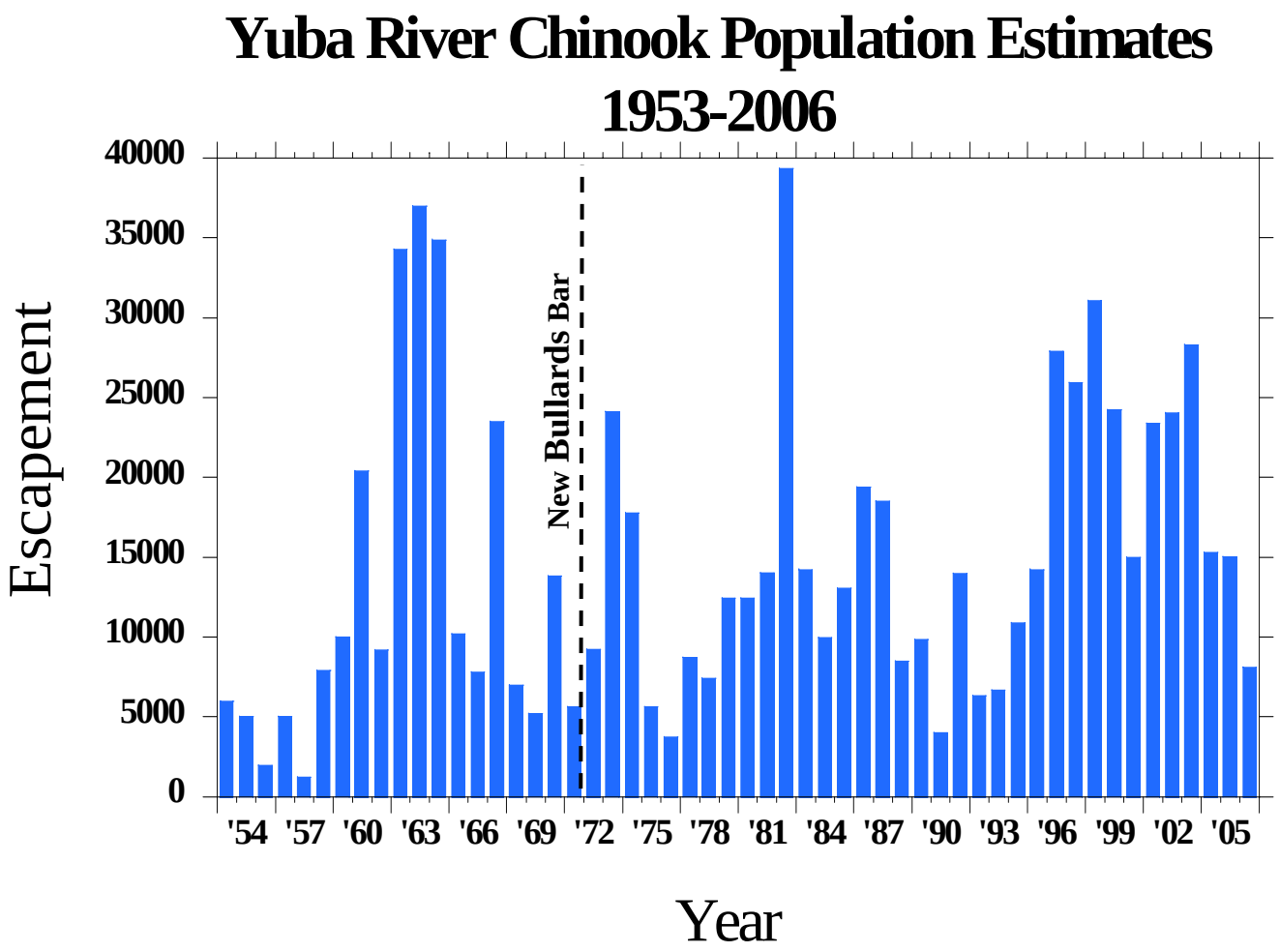

Figure 5. Inter-decadal fluctuations of Chinook salmon escapement on the Yuba River, CA between 1953 and 2006.

A)

B)

Figure 6. The bedrock channel EDR below Englebright dam at ~33.7 cms (A) and the gravel-bed TBAR reach at a discharge of ~22.5 cms (B). The coarse floodplain at the EDR is composed of rock blasted from surrounding hillsides during the construction of Englebright. The gravel bed TBAR site lacks large clusters of blast rock and is composed of alluvial hydraulic mine debris.

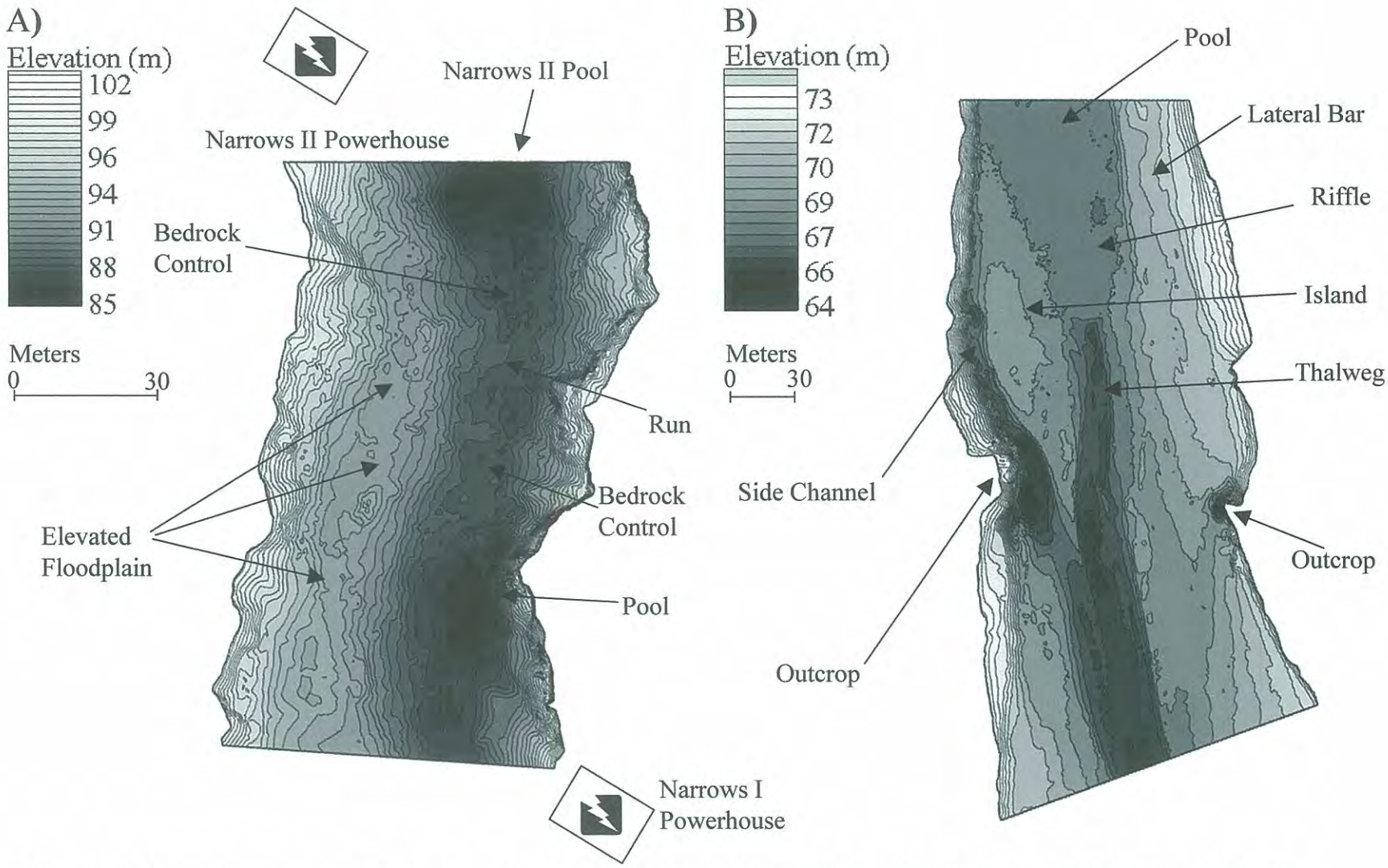

Figure 7. Digital elevation maps of A) the confined bedrock channel at the EDR and B) the alluvial TBAR on the Yuba River, CA. Contour intervals represent 0.5 meters.

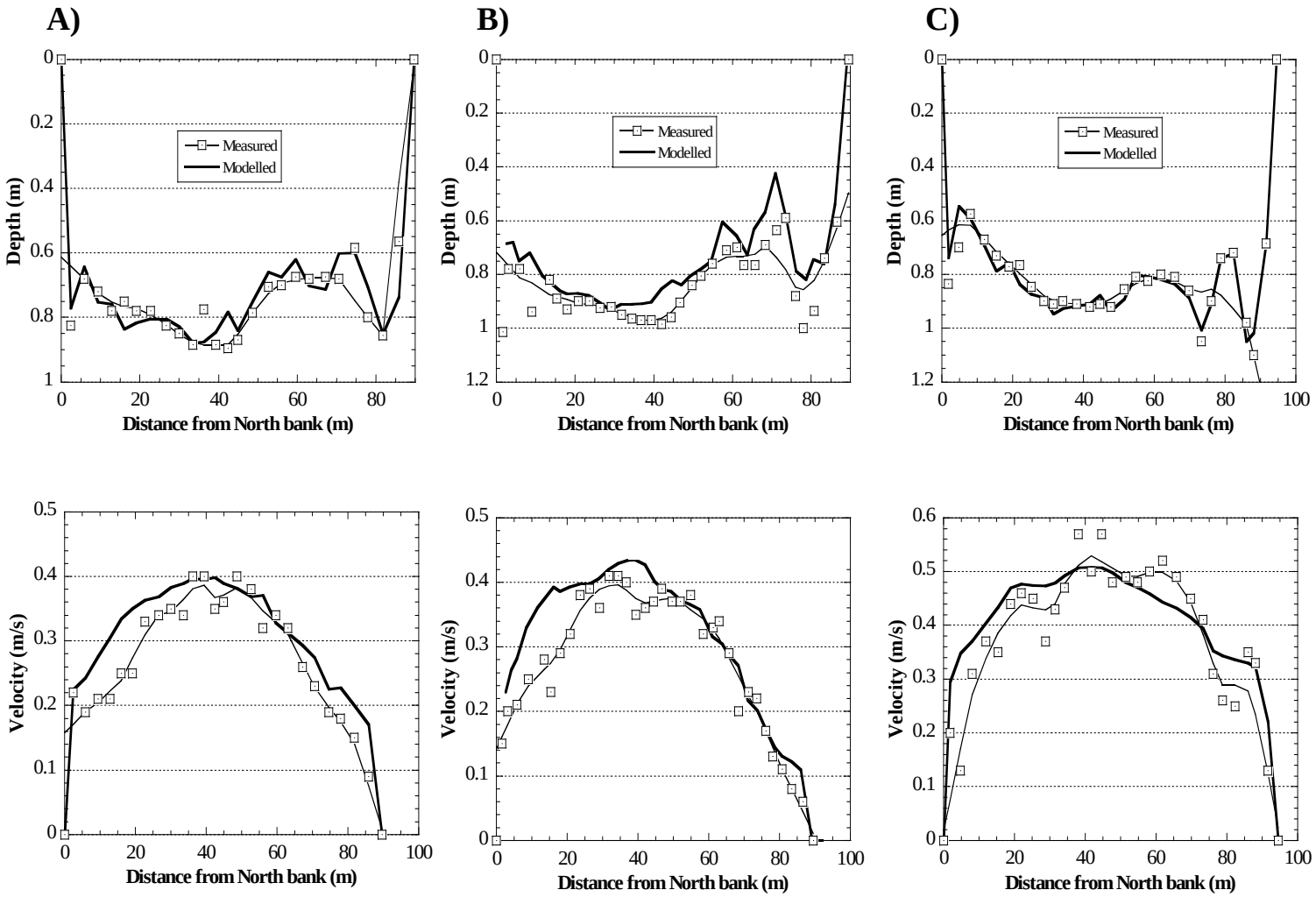

Figure 8. Field measurements and model predictions of depth and velocity at three cross sections during an A) 18.40 cms, B) 21.15 cms, and C) 31.18 cms discharge event at the TBAR site.

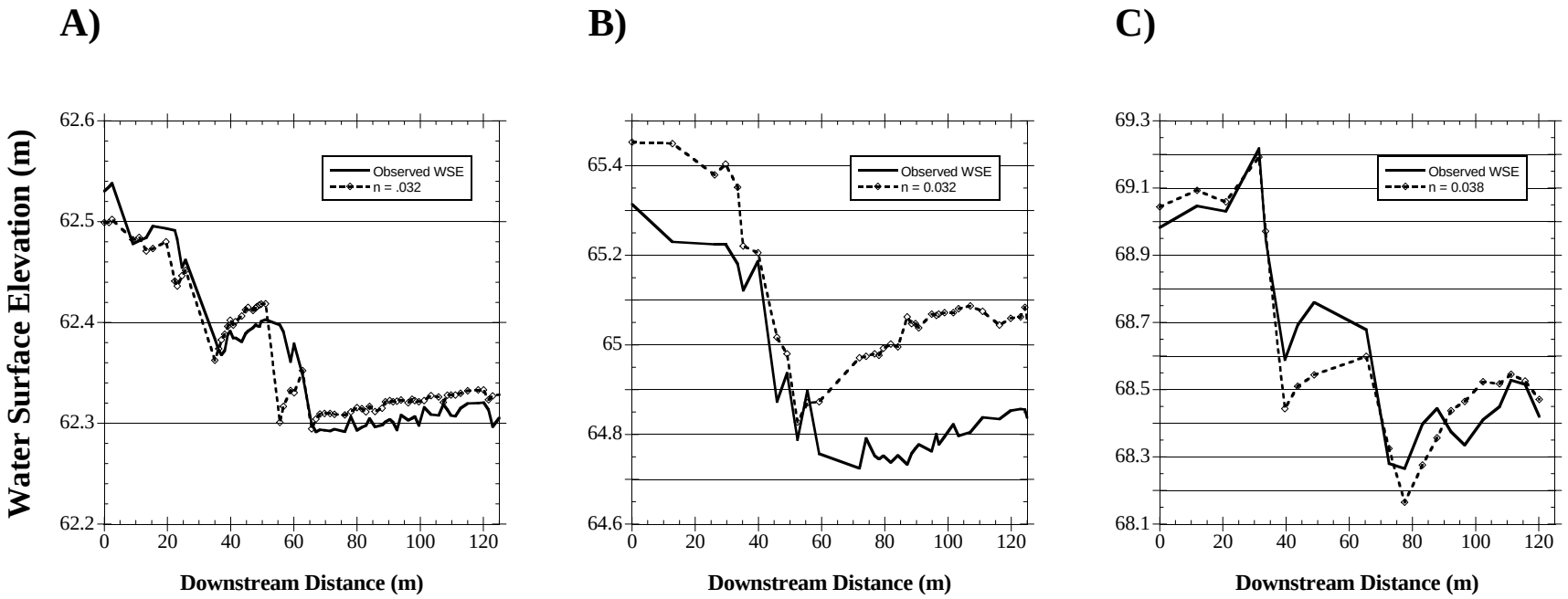

Figure 9. Measured and modeled water surface profiles for the A) 33.7 cms B) 271.3 cms, and C) 900.5 cms discharge events at the EDR. Datum corresponds to most upstream water surface elevation point measured in the field.

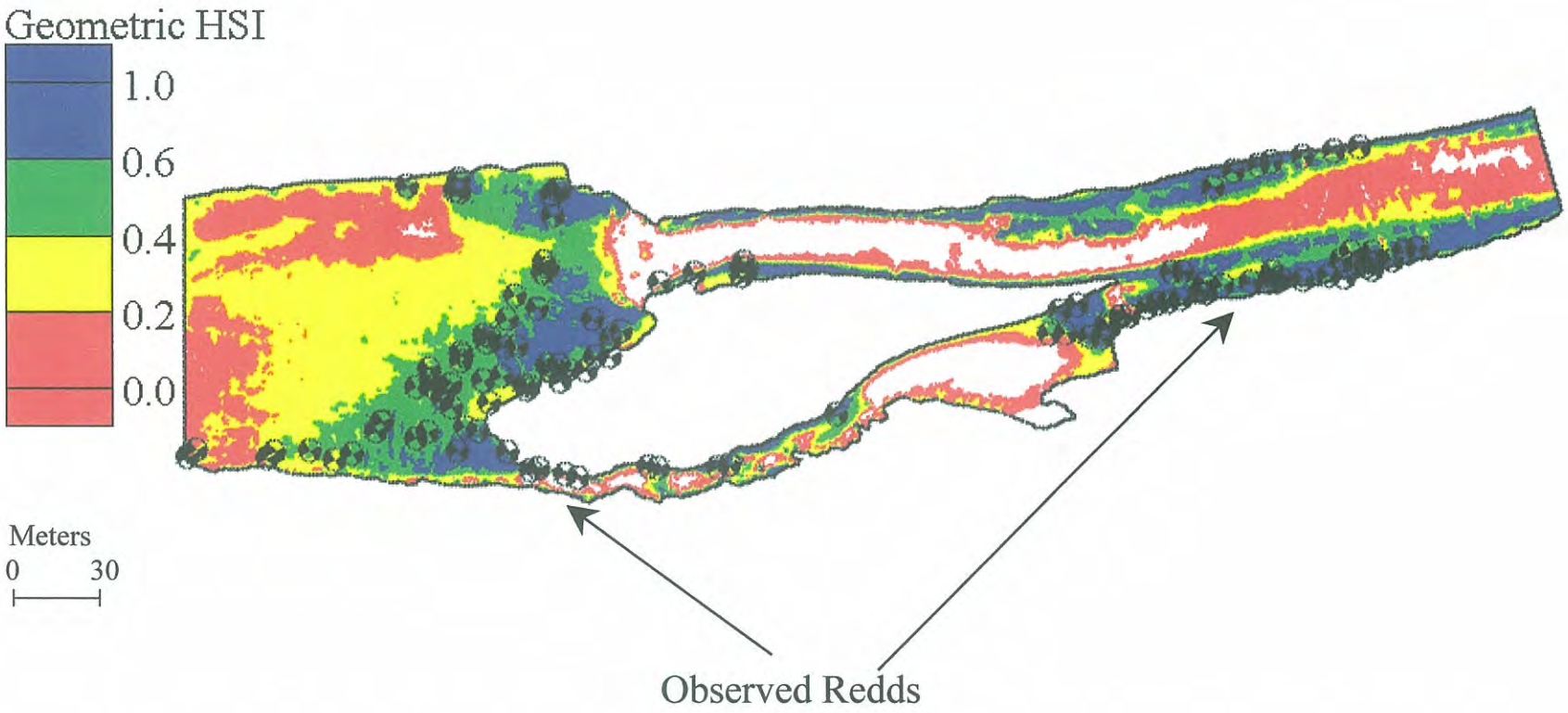

Figure 10. The spatial distribution of model predicted GHSI values and field observed redds for the 21.1 cms discharge at the TBAR.

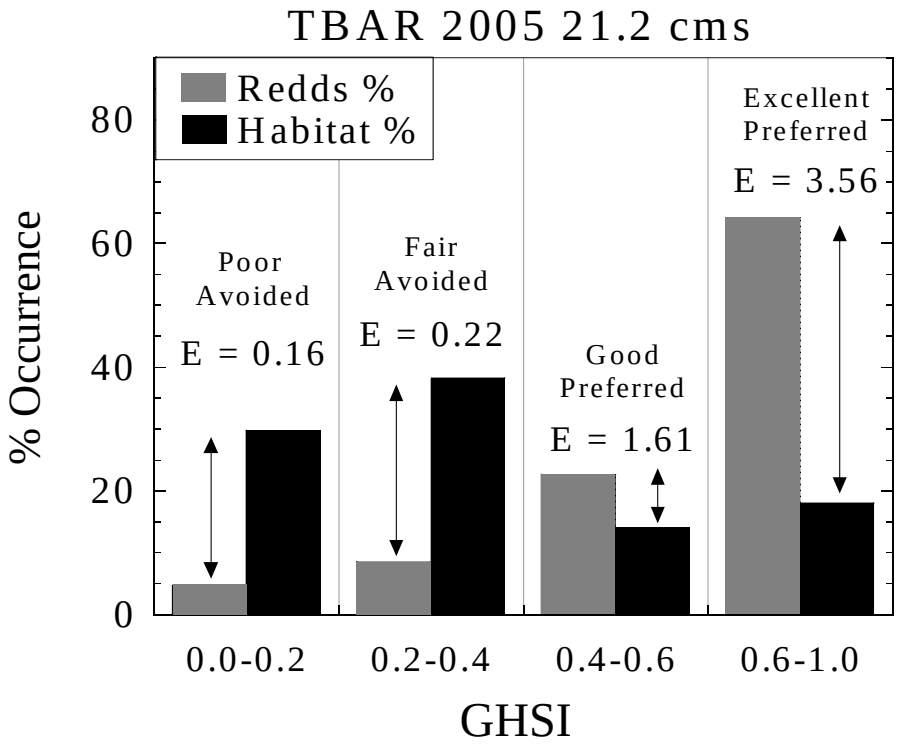

Figure 11. The percent of observed redds and model predicted habitat in each of the GHSI classes at the 2005 TBAR. Redds were observed at flows near ~22 cms and the modeled discharge for habitat predictions was 21.2 cms.

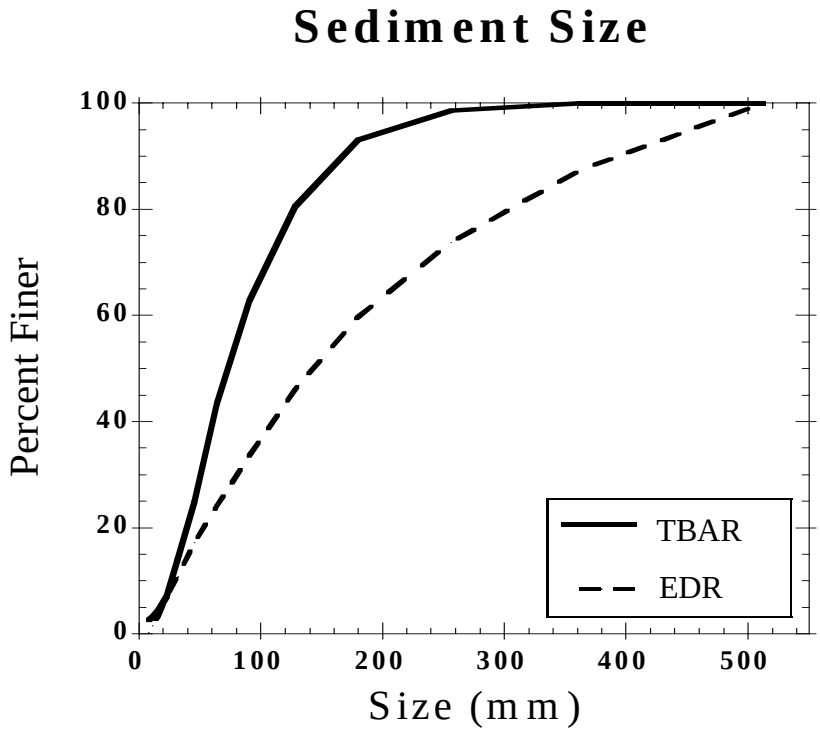

Figure 12. Cumulative frequency plot of pebble counts at the TBAR and EDR.

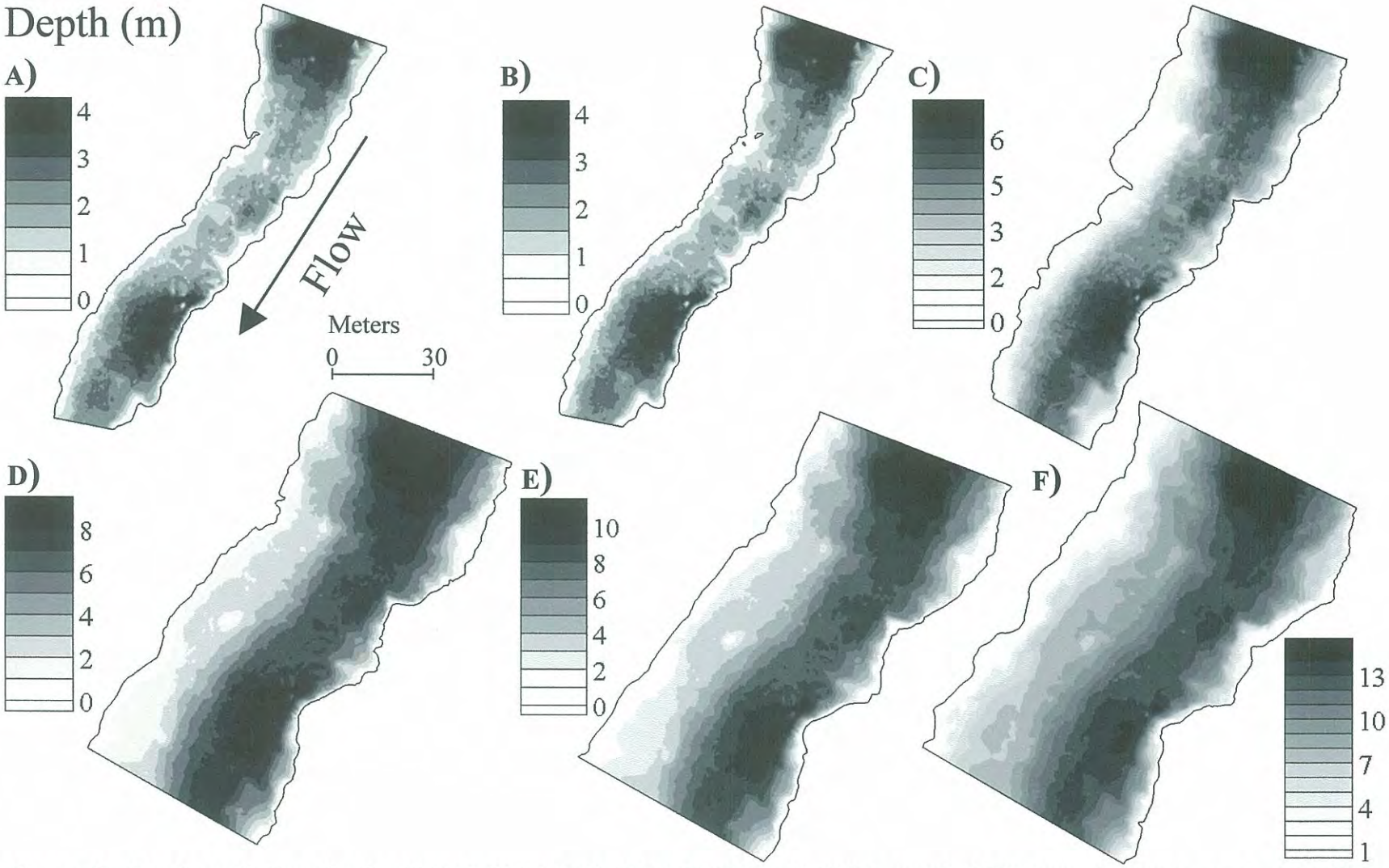

Figure 13. Depth predictions for the A) 22.7, B) 33.7, C) 271.3, D) 710.7, E) 900.5, and F) 2588.2 cms discharge events at the EDR.

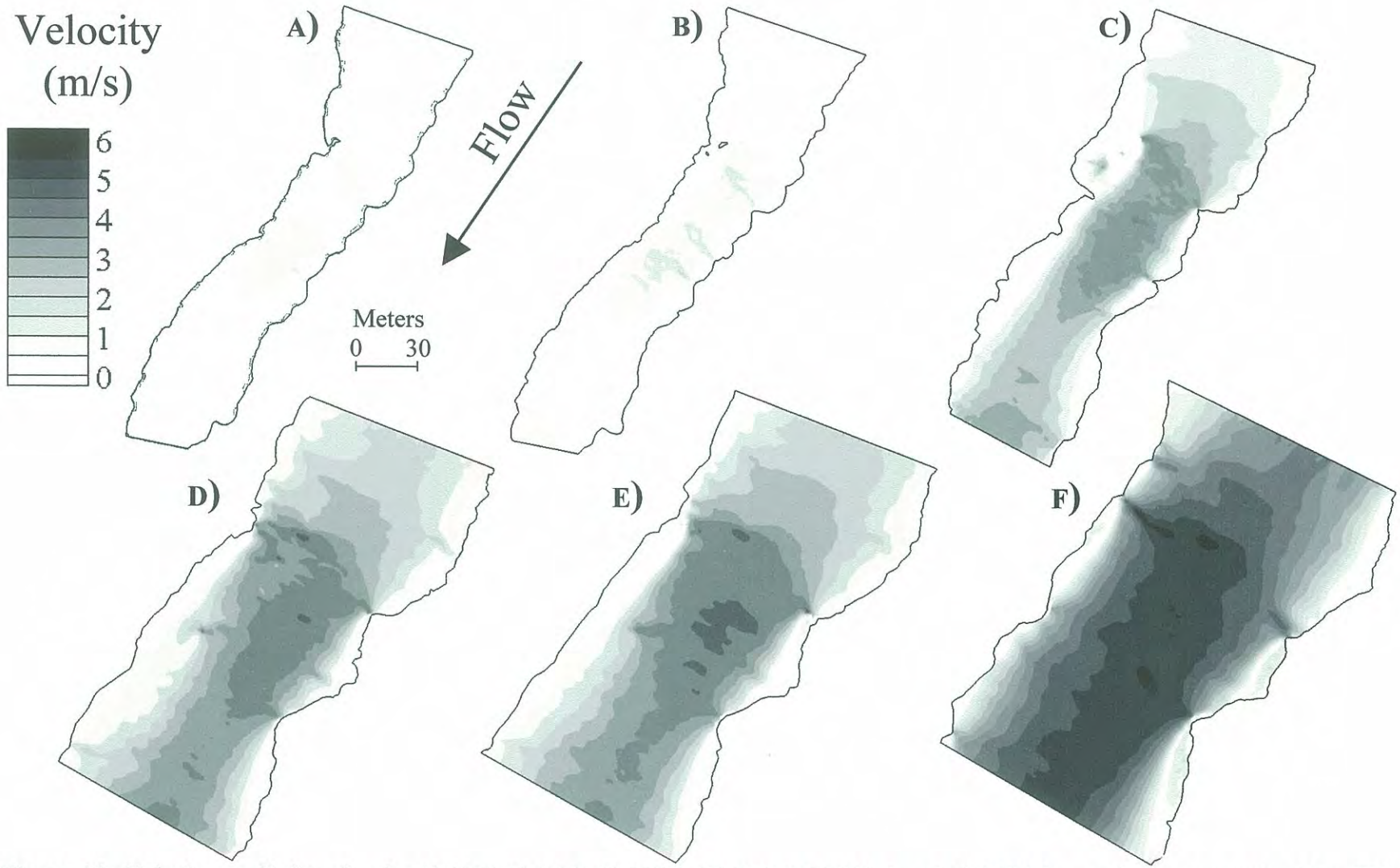

Figure 14. Velocity predictions for the A) 22.7, B) 33.7, C) 271.3, D) 710.7, E) 900.5, and F) 2588.2 cms discharge events at the EDR.

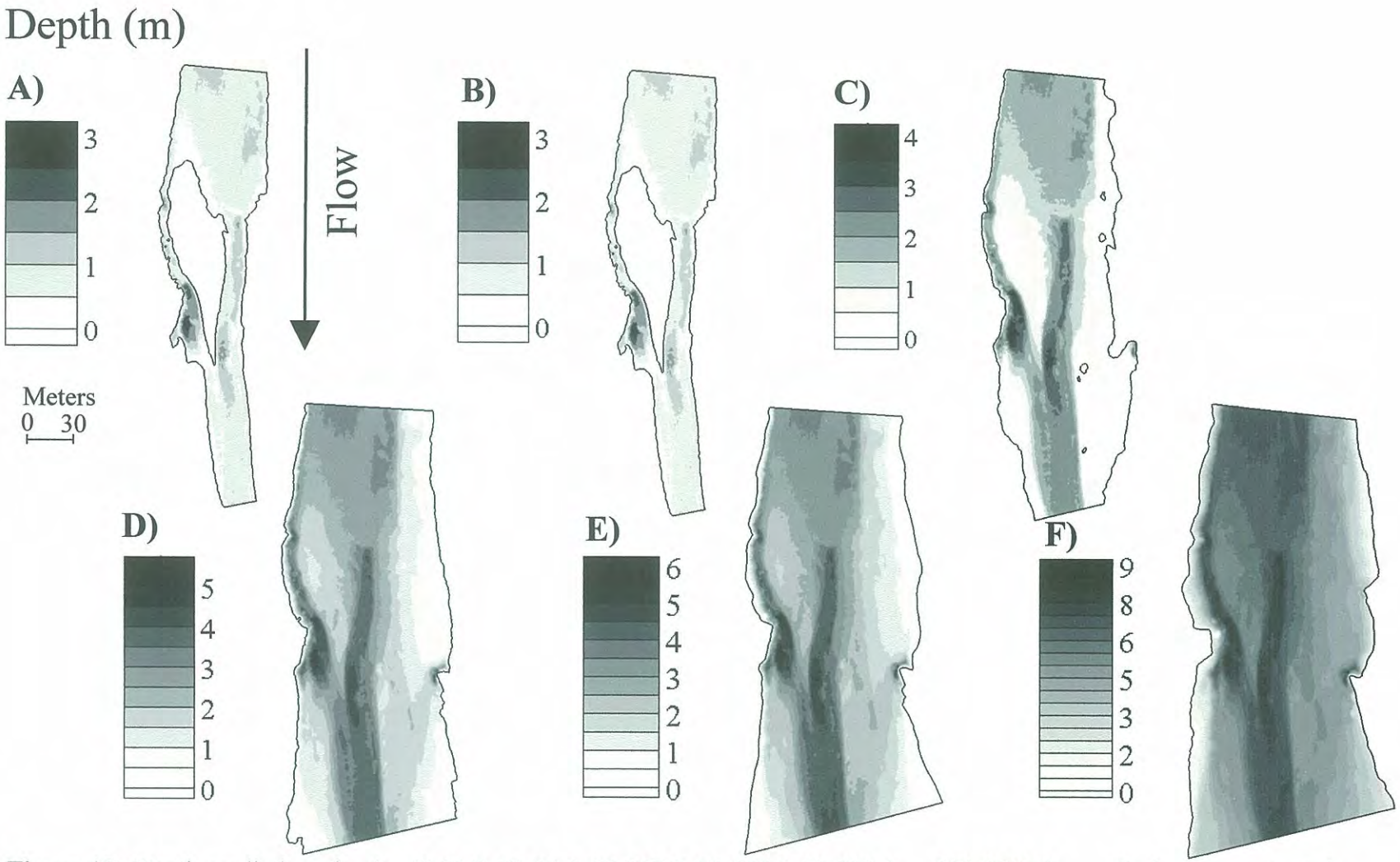

Figure 15. Depth predictions for the A) 21.2, B) 34.6, C) 267.8, D) 655.3, E) 998.4, and F) 3089.2 cms discharge events at the TBAR.

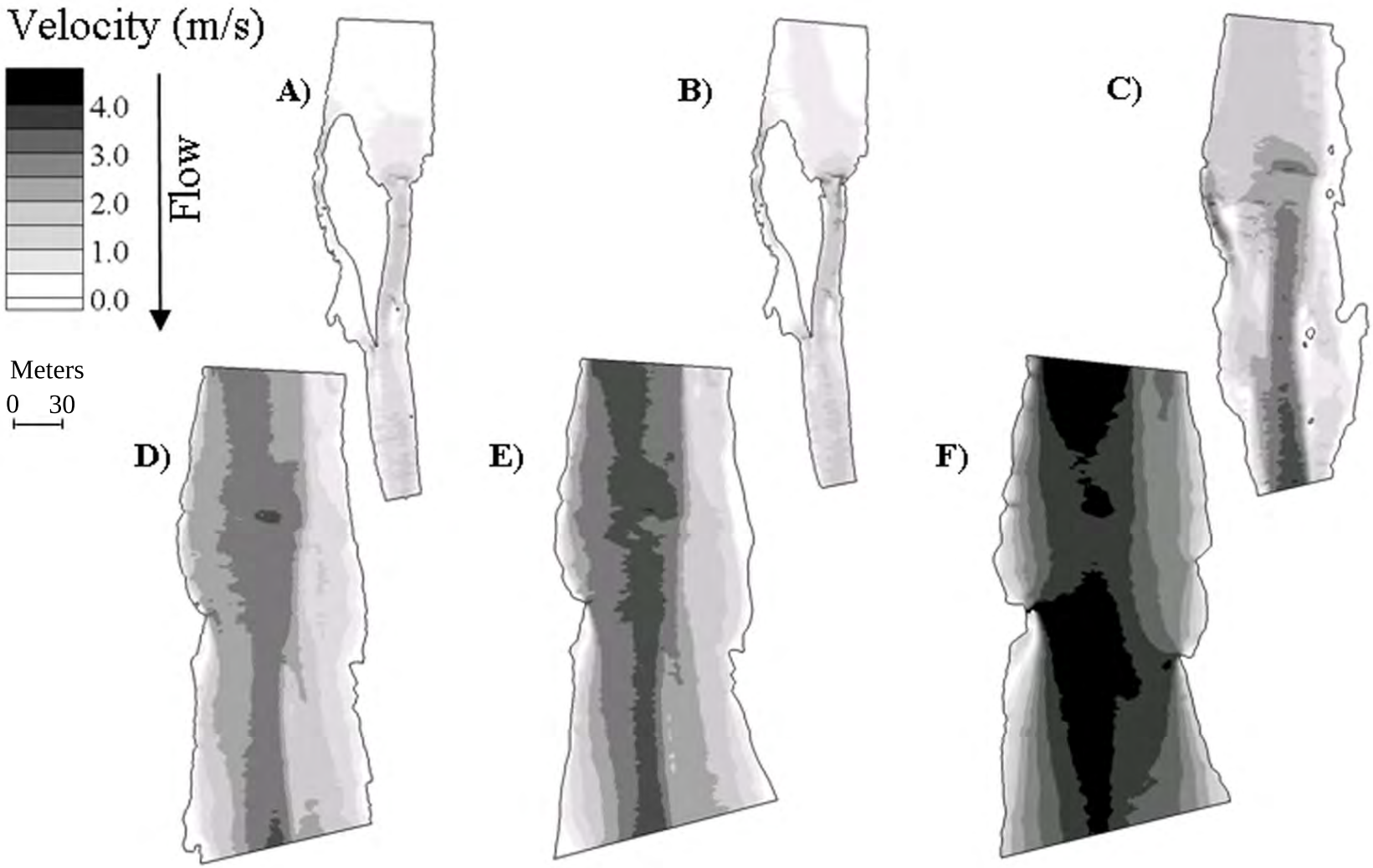

Figure 16. Velocity predictions for the A) 21.2, B) 34.6, C) 267.8, D) 655.3, E) 998.4, and F) 3089.2 cms discharge events at the TBAR.

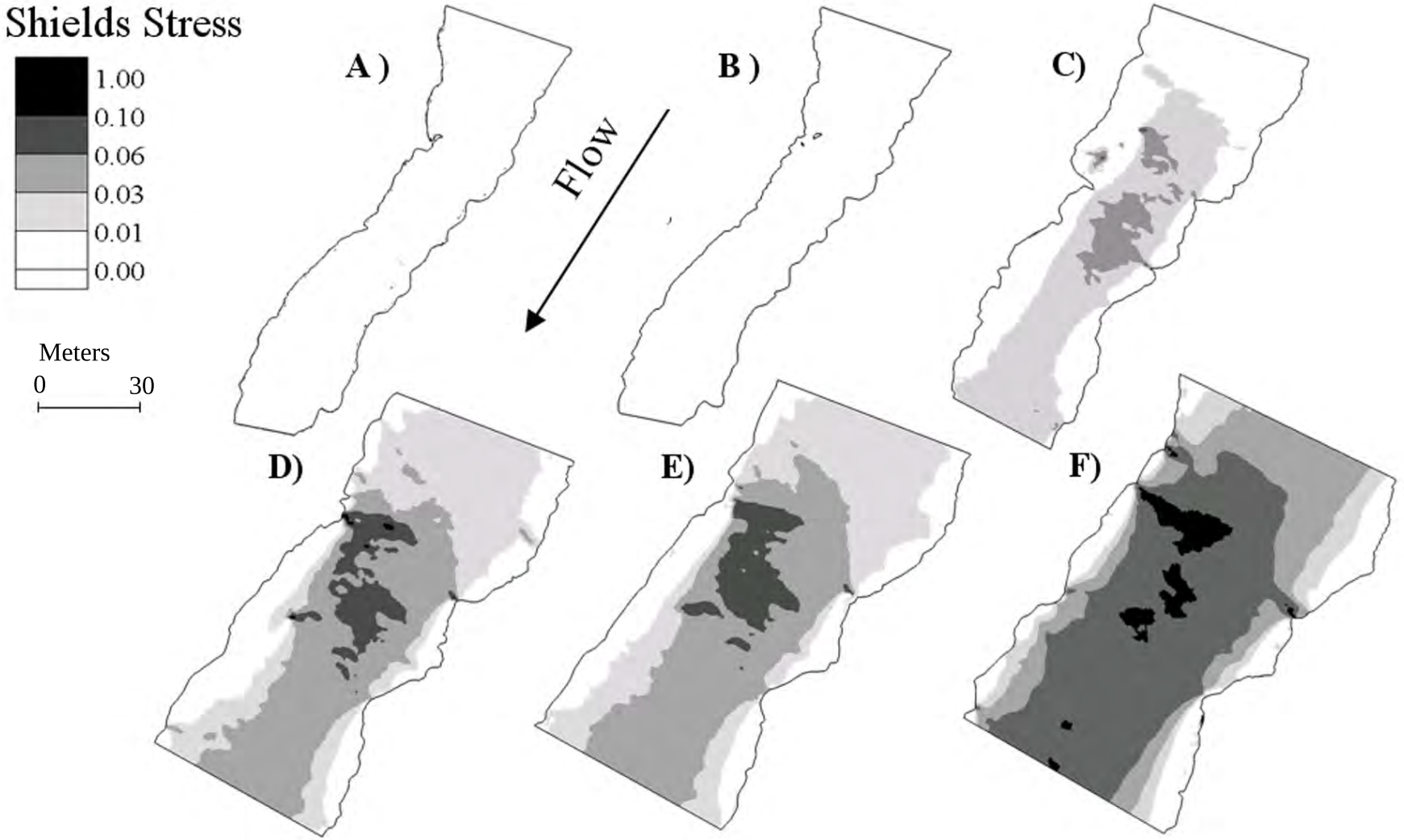

Figure 17. Shields stress predictions for the A) 22.7, B) 33.7, C) 271.3, D) 710.7, E) 900.5, and F) 2599.2 cms discharge events at the EDR.

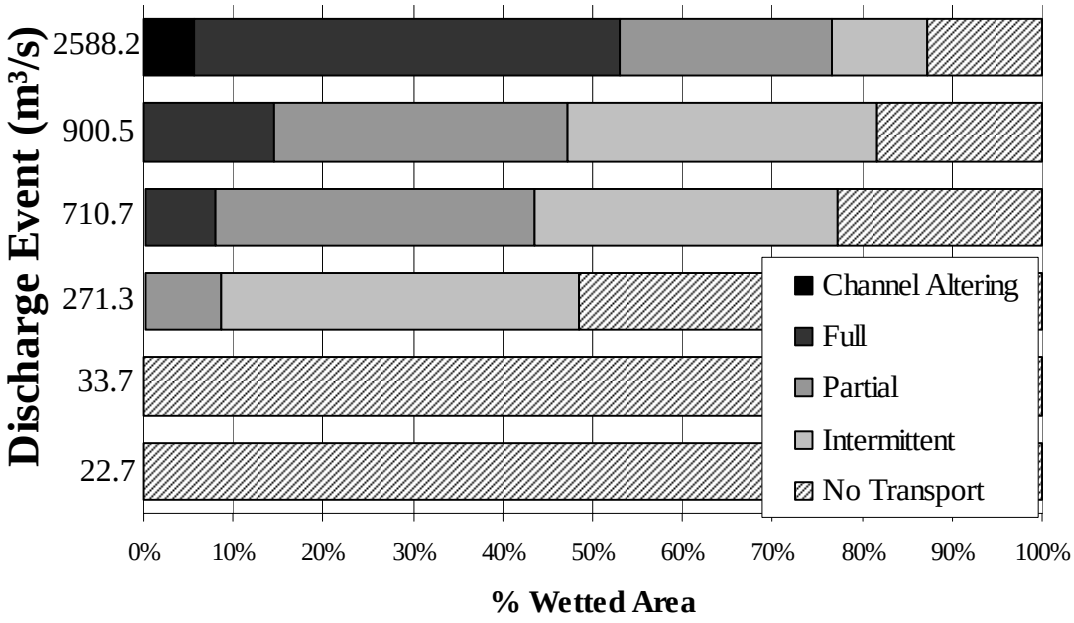

Figure 18. Percent of wetted channel area in representative Shields stress classes at the EDR for all modeled flow scenarios.

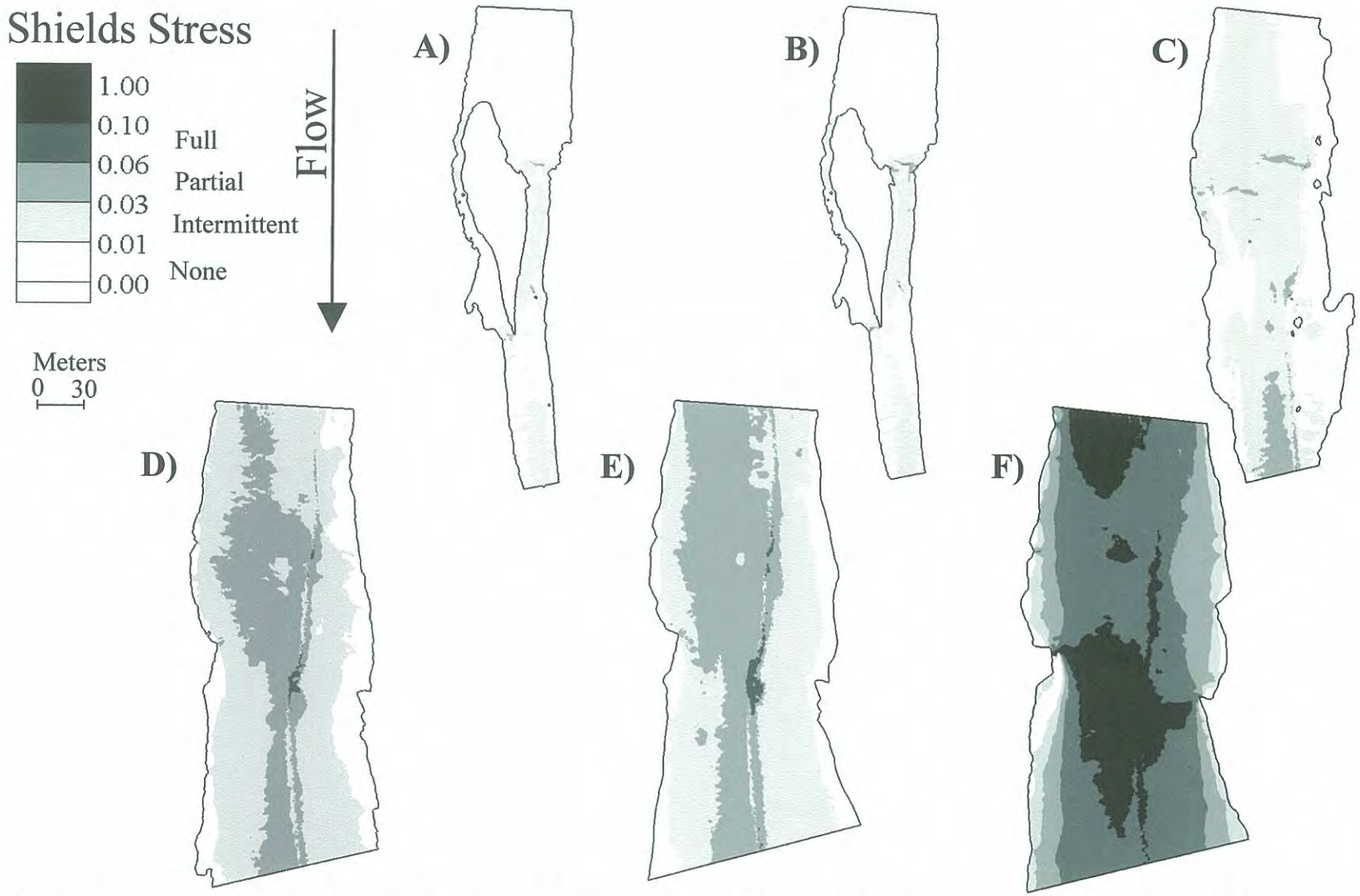

Figure 19. Shields' stress predictions for the A) 21.2, B) 34.6, C) 267.8, D) 655.3, E) 998.4, and F) 3089.2 m^3/s discharge events at the TBAR.

Figure 20. Historical photograph of the main-stem Yuba River 0.4 km upstream of the EDR study site (G.K. Gilbert; *USGS, 1909)*. Note presence of small riffle on river left, and localized deposits of sediment clustered near bedrock and roughness elements along channel margins (river right).

Figure 21. A steam shovel, dump truck, and five wagon drills razed the weathered canyon hillsides on July 25th 1939 at the EDR. Large quantities of rock were stockpiled to support construction roads along channel margins and were later transported during high flow events (Courtesy: USACE, 2006).

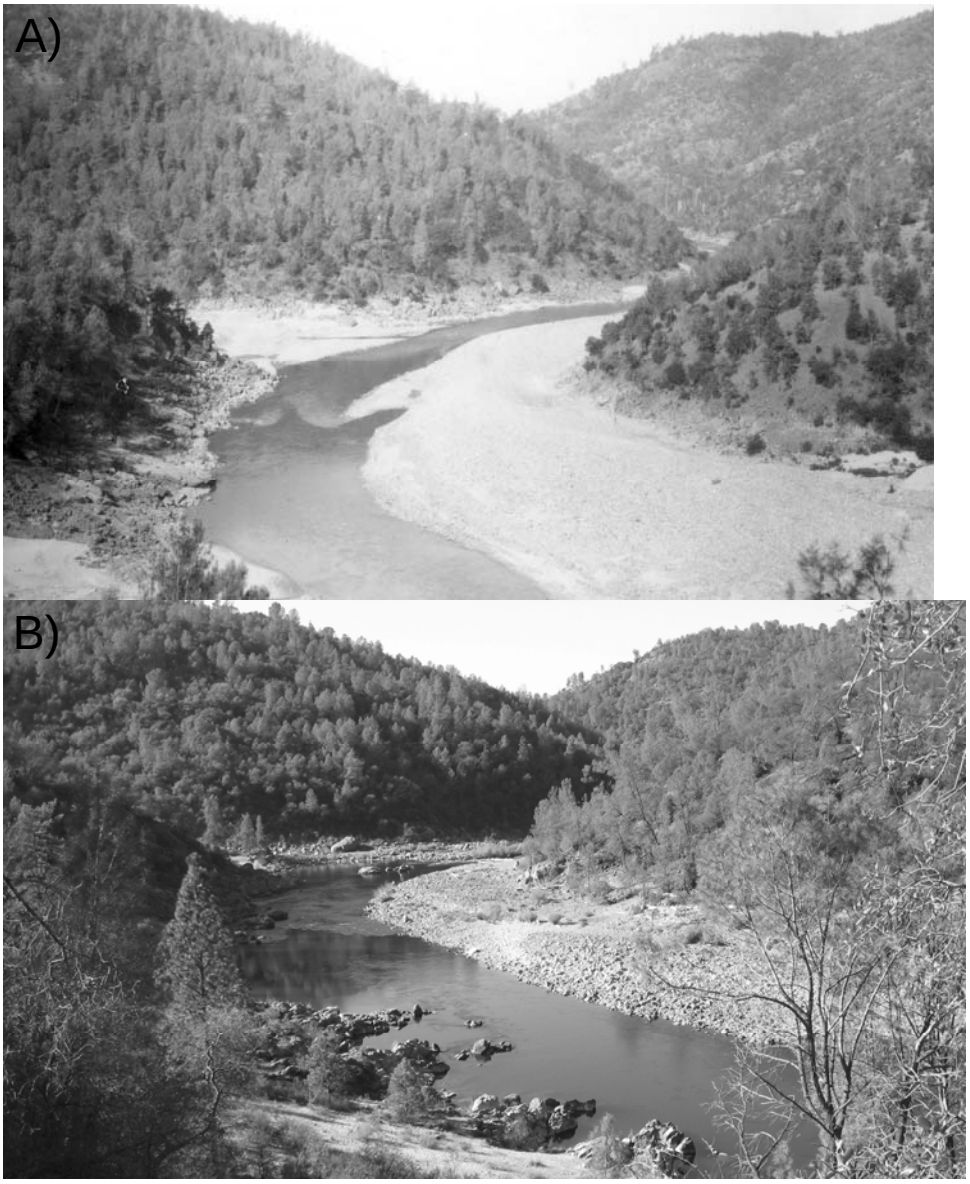

Figure 22. Imagery obtained by G.K. Gilbert of the Deer Creek confluence in 1909 (A) and a recent photo in 2006 (B) of the same location. Both images are located ~ 0.5 km downstream of the EDR where Deer Creek joins the mainstem Yuba River.

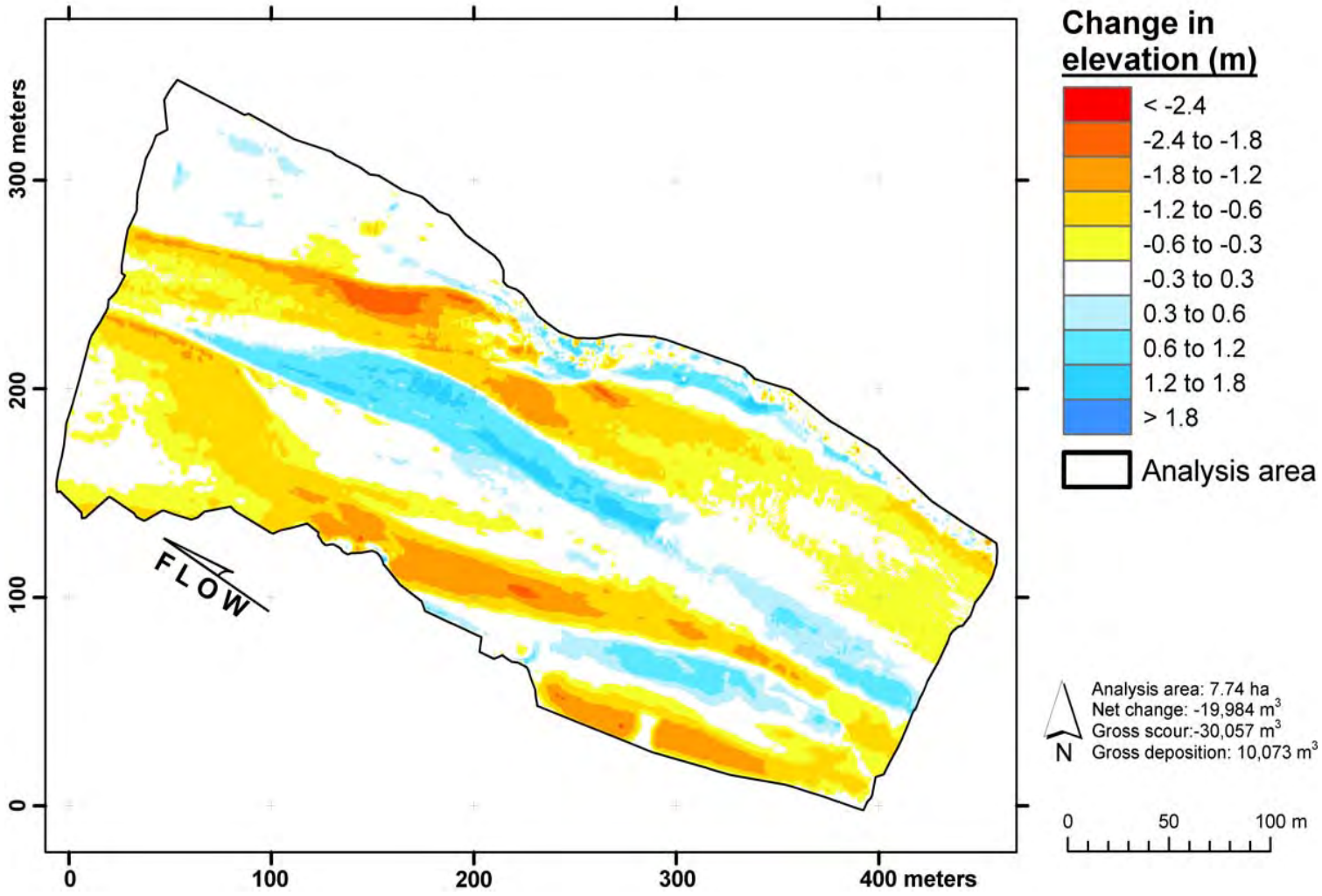

Figure 23. Patterns of scour depths (negative values) and fill heights (positive values) at the TBAR following the 3089 cms event. (Figure produced by S. Morford)

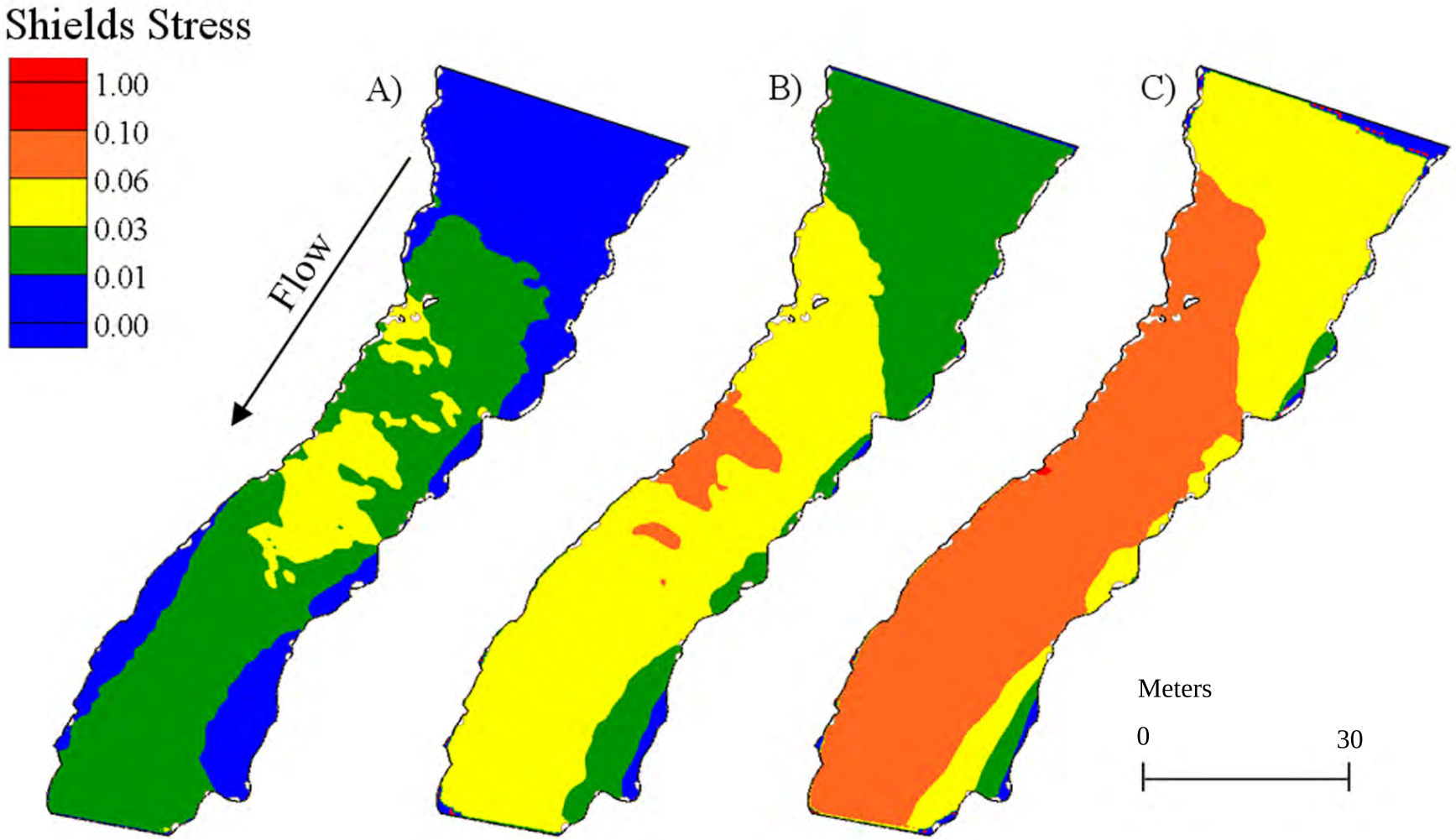

Figure 24. Shields stress predictions for a discharge of A) 271.3 cms (2-yr event), B) 900.5 cms (5-yr event) and C) 2588.2 cms (24-yr event) in the EDR spawing channel (33.7 cms wetted channel area).

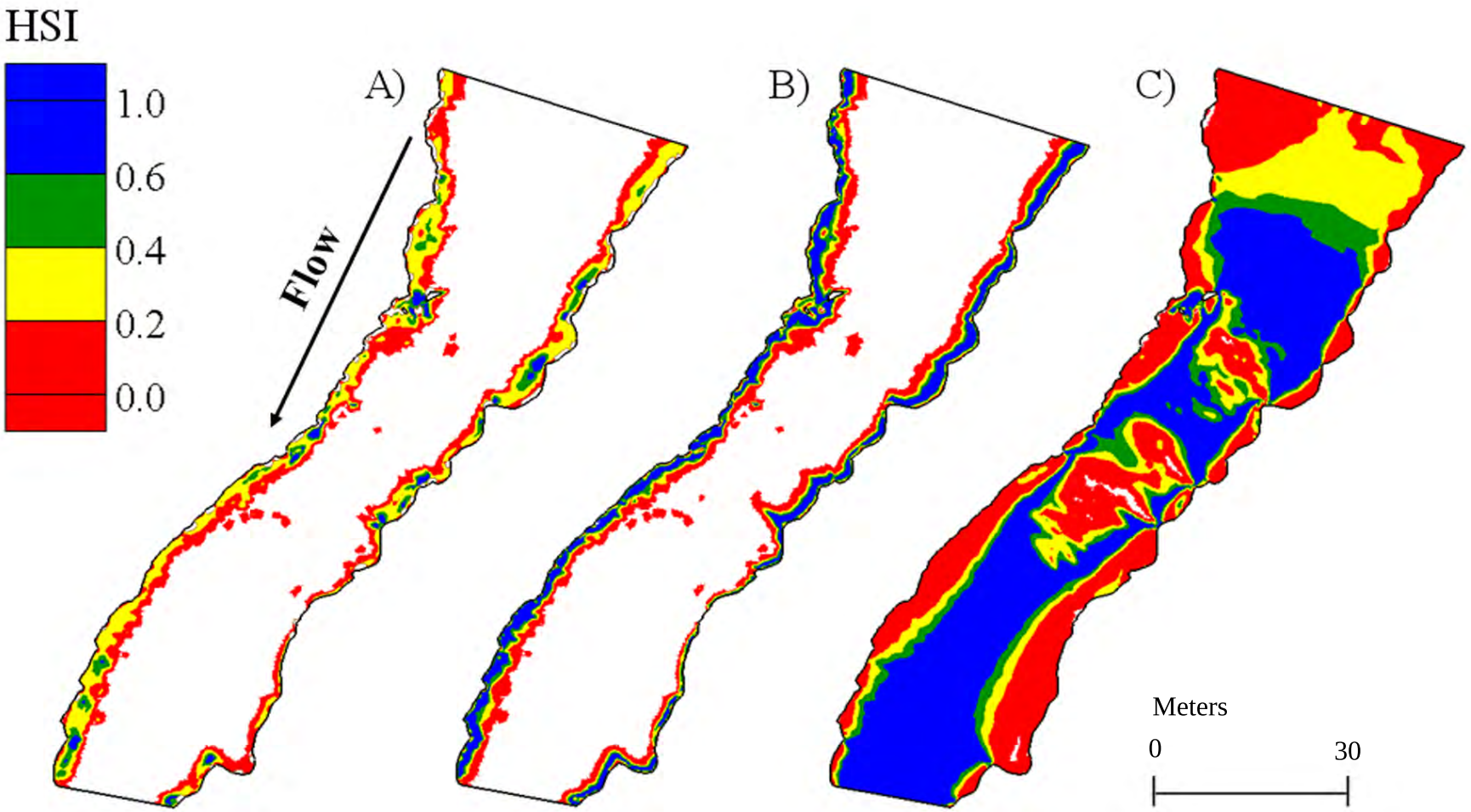

Figure 25. Model predictions of the A) geometric habitat suitability index (GHSI), B) depth habitat suitability index (DHSI), and C) velocity habitat suitability index (VHSI) for the 33.7 cms spawning flow at the EDR.

Hyp.	Statement	Test Metrics *
H_1	Sediment characteristics at the EDR and TBAR are comparable and suitable for spawning.	PC, VC, LR
H_2	Flow convergence routing will produce alluvial geomorphic features (riffles, pools, glides) at the EDR and TBAR study sites.	HM, SS
H_3	Injected gravels at the EDR will be stable during spawning flows.	HM, SS
H_4	Injected gravels at the EDR will be stable during 273.2 m^3/s discharges (~2-year event).	HM, SS
H_5	Injected gravels at the EDR will be stable during a 900.5 m^3/s discharge (~5-year event).	HM, SS
H_6	Injected gravels at the EDR will be stable during a 2588.2 m^3/s discharge (~24-year event).	HM, SS
H_7	Gravel augmentation will aggrade the EDR and produce extensive cross channel habitat	HM, SS, HI, DR
H_8	Historically, the EDR supplied ample spawning habitat for chinook salmon.	HI, LR, HOS, ROS
H_9	Current spawning habitat at the EDR and TBAR is not limited.	HM, HSC

* DR = Discharge Record Analysis, HI = Historical Imagery, HM = Hydraulic Modeling, HSC = Habitat Suitability Curves, LR = Literature Review, PC = Pebble Counts, HOS = Historical Observations of Spawning, SS = Shields Stress Predictions, ROS = Recent Observations of Spawning, VC = Visual Comparisons

Table 1. Hypotheses and test metrics used for evaluating the efficacy of gravel augmentation at the bedrock channel EDR.

Location	Discharge (m^3/s)	Downstream WSE (m)	Manning's *n*
TBAR	21.2	66.35	0.03
	34.6	66.53	0.03
	267.8	67.95	0.03
	655.3	69.51	0.03 & 0.052
	998.4	70.22	0.03 & 0.053
	3089.2	72.83	0.03 & 0.054
EDR	22.7	62.20	0.032
	33.7	62.30	0.032
	271.3	64.82	0.032
	710.7	67.32	0.038
	900.5	68.45	0.038
	2588.2	72.83	0.038

Table 2. FESWMS model inputs for the six comparable flows included downstream water surface elevation, Manning's *n* , and gaged discharge at the EDR and TBAR sites.

Discharge (m^3/s)	33.7 m^3/s (n=75)			900.5 m^3/s (n=20)		
Manning's n	Mean Error (m)	σ	Ev (m^2/s)	Mean Error (m)	σ	Ev (m^2/s)
0.022	0.028	0.020	0.8	-	-	-
0.024	0.022	0.024	0.8	-	-	-
0.026	0.021	0.021	0.8	-	-	-
0.028	0.022	0.021	0.8	-	-	-
0.03	**0.020**	0.018	0.8	0.103	0.088	2.5
0.032	**0.020**	0.015	0.4	0.097	0.086	2.5
0.034	**0.020**	0.013	0.4	0.086	0.082	2.5
0.036	0.022	0.013	0.4	0.085	0.077	2.5
0.038	0.025	0.013	0.4	**0.081**	0.056	2.5
0.04	0.028	0.013	0.4	0.086	0.063	2.5

Table 3. Mean errors, standard deviation of errors, and corresponding eddy viscosity values for Manning's *n* calibration scheme at the EDR. Bold values represent the smallest absolute error obtained in the analysis.